Matrikines are key regulators in modulating the amplitude of lung inflammation in acute pulmonary infection

Samia Akthar[1], Dhiren F. Patel[1], Rebecca C. Beale[1], Teresa Peiró[1], Xin Xu[2], Amit Gaggar[2,3,4], Patricia L. Jackson[2], J. Edwin Blalock[2,4], Clare M. Lloyd[1], Robert J. Snelgrove[1].

[1]Leukocyte Biology Section, National Heart and Lung Institute, Imperial College London, London, SW7 2AZ, United Kingdom.

[2]Division of Pulmonary, Allergy and Critical Care Medicine, University of Alabama at Birmingham and Lung Health Center, Department of Medicine, University of Alabama at Birmingham, Birmingham, AL 35294.

[3]Gregory Fleming James Cystic Fibrosis Center and Program in Protease and Matrix Biology, University of Alabama at Birmingham, Birmingham, AL 35294.

[4]Birmingham V.A. Medical Center, Birmingham, AL 35294

Corresponding author: Robert J. Snelgrove
Tel: 0207 594 8192
robert.snelgrove@imperial.ac.uk

Abstract

Bioactive matrix fragments ("matrikines") have been identified in a myriad of disorders but their impact on the evolution of airway inflammation has not been demonstrated. We recently described a pathway where the matrikine and neutrophil chemoattractant proline-glycine-proline (PGP) could be degraded by the enzyme leukotriene A_4 hydrolase (LTA_4H). LTA_4H classically functions in the generation of pro-inflammatory leukotriene B_4, thus LTA_4H exhibits opposing pro- and anti-inflammatory activities. The physiological significance of this secondary anti-inflammatory activity remains unknown. Here we show, using readily resolving pulmonary inflammation models, that loss of this secondary activity leads to more pronounced and sustained inflammation and illness owing to PGP accumulation. PGP elicits an exacerbated neutrophilic inflammation and protease imbalance that further degrades the extracellular matrix, generating fragments that perpetuate inflammation. This highlights a critical role for the secondary anti-inflammatory activity of LTA_4H and thus has consequences for the generation of global LTA_4H inhibitors currently being developed.

Introduction

Neutrophils are critical components of the body's immune response, being readily mobilized to the site of infection and destroying invading micro-organisms[1, 2]. Recruitment of neutrophils into the tissue in response to infection is mediated by an array of chemoattractant signals, including lipid molecules such as leukotriene B_4 (LTB_4) and the glutamic acid-leucine-arginine$^+$ (ELR^+) class of chemokines. ELR^+ chemokines, including IL-8 in humans and KC and MIP-2 in mice, exert their activity by binding to receptors CXCR1/2[3]. Despite their clear antimicrobial capacity, neutrophils are not indiscriminate killers but their inflammation is tightly regulated and they are able to elegantly and specifically shape many facets of the elicited immune response[4, 5]. However, owing to their potent arsenal, an over-exuberant or persistent neutrophilic inflammation is implicated in the pathologies of chronic diseases such as chronic obstructive pulmonary disease (COPD) and cystic fibrosis (CF)[6, 7].

A protease-antiprotease imbalance is a hallmark of many chronic lung diseases, with the presence and activity of several matrix metalloproteinases (MMPs) and neutrophil elastase (NE), in particular, correlating with COPD pathology. Such proteases target the extracellular matrix (ECM) for degradation, disrupting tissue architecture and releasing ECM-derived chemoattractant signals, termed 'matrikines', that can perpetuate inflammation[8]. Models of exposure to cigarette smoke show that both breakdown of ECM (by neutrophil or macrophage elastase) and accumulation of neutrophils are required for pathological changes[9-12]. It is plausible therefore that a protease/matrikine driven inflammation may underlie the pathology observed in such chronic diseases.

The tripeptide Proline-Glycine-Proline (PGP) is one such matrikine, being a neutrophil chemoattractant derived from ECM collagen that exerts its activity by mimicking key sequences found in ELR^+ chemokines and binding to CXCR1/2[13]. PGP is generated from collagen via the sequential enzymatic activity of MMPs (specifically MMP-8 and -9) and prolylendopeptidase (PE) [14]. Significant quantities of PGP are found in patients with chronic lung diseases such as COPD, CF and bronchiolitis obliterans syndrome (BOS)[14-18]. Recently, we have identified a novel anti-inflammatory pathway whereby PGP is readily degraded by the extracellular activity of the enzyme leukotriene A_4 hydrolase (LTA_4H)[19]. We subsequently demonstrated that this

LTA_4H-mediated PGP degradation is perturbed by cigarette smoke, contributing to the accumulation of PGP in COPD[18, 19].

LTA_4H is classically recognized for its intracellular epoxide hydrolase activity whereby it generates the pro-inflammatory lipid mediator LTB_4[20, 21]. LTB_4 may bind to receptors BLT1 or BLT2 - whilst BLT1 is a high affinity and specific receptor for LTB_4, BLT2 binds LTB_4 with substantially lower affinity and can also bind to other eicosanoids[22]. The physiological functions of LTB_4 are attributed to signaling through BLT1. LTB_4 can drive the recruitment and activation of an array of cells including neutrophils and is thus implicated in protection against invading micro-organisms but also in the pathology of an array of diseases[23-27]. Thus LTA_4H represents an unusual enzyme with opposing pro- and anti-inflammatory activities that dictate the amplitude and persistence of neutrophilic inflammation[28]. There has been significant interest from pharmaceutical companies to target LTA_4H therapeutically to alleviate LTB_4-mediated pathologies, but despite the generation of several excellent inhibitors, these drugs have failed to demonstrate clinical efficacy[29, 30]. The lack of success of these compounds could feasibly be due to their failure to distinguish between the opposing roles of LTA_4H and thus inadvertently prevent PGP degradation.

The critical role of LTA_4H in generating LTB_4 and the significance of this lipid mediator in multiple inflammatory settings are undeniable. Whilst it's clear that LTA_4H possesses a secondary anti-inflammatory role in degrading PGP, the relative physiological significance of this activity remains unclear. To address this we have manipulated the LTA_4H pathways in a murine model of *Haemophilus influenza*e b (Hib). *Haemophilus influenzae* is a Gram-negative coccobacillus, of which there are encapsulated and unencapsulated strains[31, 32]. Unencapsulated strains are termed non-typeable (NTHI) and are frequent causes of exacerbations of COPD and asthma. Encapsulated strains are divided into serotypes, of which there are six (a-f), based on their capsular antigen. Serotype B (Hib) is the cause of most invasive *H. influenzae* infections, which include pneumonia, meningitis, septicaemia and epiglottitis[33]. However, in most people Hib is found as a commensal of the nasopharynx, with the bacteria becoming invasive in only a small number of cases.

The murine model of Hib infection was chosen to dissect the dual activities of LTA_4H since it represents a non-complicated infection whereby the pathogen is readily cleared but elicits a

robust pulmonary neutrophilia that is rapidly resolved. In this setting, it is feasible to address whether a failure to degrade PGP can lead to an augmented and prolonged neutrophilia to what is a relatively innocuous pulmonary insult. It thus provides an ideal model to probe the relative roles of LTB_4 and PGP in protection and pathology. In this context, LTB_4 was shown to be critical to bacterial phagocytosis and killing on a per cell basis but did not control the magnitude of the inflammatory response or illness. Conversely, a failure of LTA_4H-mediated degradation of PGP led to accumulation of the peptide and a dramatic augmentation in inflammation and illness. This manifested primarily as a PGP-mediated increase in neutrophil numbers in the lung and airways and a secondary protease imbalance that resulted in generation of elastin-derived matrikines that promoted a secondary macrophage infiltrate. Thus the failure to degrade PGP can have significant deleterious consequences, highlighting the key physiological role of the secondary anti-inflammatory activity of LTA_4H and the prominent pathological role of PGP in inducing a general protease-matrikine imbalance.

Results

Dual LTA_4H activities are functional during Hib infection.

Infection of 129/S6 mice with Hib elicited a transient, mild weight loss peaking at 24-48 hrs post infection, which correlated with the size of inoculating dose of bacteria (Fig. 1A). Coinciding with peak illness was a robust, readily resolving inflammation observed in the airways (Fig. 1B) and lungs (Fig. 1C). Consequently, bacteria were promptly cleared from the airways (Fig. 1D) and lung parenchyma (Fig. 1E) of infected mice. The pulmonary infiltrate was predominantly neutrophilic, with Hib inducing a rapid, dose-dependent, influx of neutrophils peaking at 24 hrs post infection (Fig. 1F and G). Secondary to this neutrophilic inflammation was a relatively modest infiltration of monocytes/macrophages, NK cells, and T cells (Supplementary Fig. 1A-E, respectively). Within this system, alveolar macrophages (Supplementary Fig. 1F-H) and neutrophils (Fig. 1H and I) were critical to the clearance of Hib since their depletion significantly compromised bacterial clearance.

The arrival of neutrophils into the lungs and airways of Hib-infected mice was preceded by the release of ELR^+ CXC chemokines KC (Fig. 1J) and MIP-2 (Fig. 1K) into the BALF. Furthermore, conventional intracellular epoxide hydrolase activity of LTA_4H was augmented by infection (Fig. 1L) and the neutrophil chemoattractant LTB_4 was released into the BALF (Fig. 1M). This elevation in epoxide hydrolase activity of LTA_4H was seemingly attributable to the substantial neutrophilic infiltrate with the activity markedly reduced following neutrophil depletion (Fig. 1N). Key PGP-generating enzymes MMP-9 (Fig. 1O and P) and PE (Fig. 1Q) were induced by Hib infection but PGP was undetectable at any time point. Neutrophils are a prominent source of these PGP-generating enzymes enabling a feed-forward vicious circle of neutrophilic inflammation[14, 19, 34-36]. Accordingly, neutrophil depletion in Hib-infected mice resulted in a significant reduction in BALF MMP-9 levels (Fig. 1R) and PE activity (Fig. 1S). The failure to detect PGP despite the presence of MMP-9/PE could be attributable to extracellular release of LTA_4H (Fig. 1T) and its capacity to degrade PGP (Fig. 1U and V). As previously postulated[19], neutrophils are likely a source of extracellular LTA_4H since their depletion resulted in reduced capacity of BALF to degrade PGP (Fig. 1W and X). Thus both the pro-inflammatory LTB_4 generating and the anti-inflammatory PGP degrading activities of LTA_4H are operational within this acute pulmonary neutrophilia model. The nature of this

elicited response to Hib observed in 129/S6 mice was comparable in Balb/c and C57BL/6 mice (Supplementary Fig. 2).

Loss of LTB_4 signaling compromises Hib clearance.

Physiological functions attributed to LTB_4 are relayed through receptor BLT1. To infer the role of LTB_4 in our Hib model, wild type (WT) and blt1-/- mice were infected with $1x10^7$ CFU of Hib. WT and blt1-/- mice displayed comparable weight loss (Fig. 2A) and inflammation into the airways (Fig. 2B) and lung parenchyma (Fig. 2C) in response to Hib. Specifically, neutrophilic inflammation into the airways (Fig. 2D) and lung tissue (Fig. 2E) was indistinguishable between Hib-infected WT and blt1-/- mice. Despite comparable cellular inflammation, clearance of Hib was compromised in blt1-/- mice at 6 (Fig. 2F) and 24hrs (Fig. 2G) post infection. A plethora of studies have highlighted the capacity of LTB_4 to augment the phagocytic and anti-microbial potential of macrophages and neutrophils on a per cell basis[26, 37-50]. Alveolar macrophages (Fig. 2H) and neutrophils (Fig. 2I) from blt1-/- mice exhibited a significant reduction in their capacity to phagocytose pHrodo-labelled Hib relative to WT controls. Furthermore, blt1-/- alveolar macrophages (Fig. 2J) and neutrophils (Fig. 2K) exhibited reduced bacterial killing of Hib on a per cell basis relative to WT counterparts.

The comparable cellular inflammation but compromised bacterial clearance observed at 24 hours post infection in Hib-infected blt1-/- mice relative to WT controls was recapitulated through administration of BLT-1 specific antagonist U-75302 to Hib-infected WT mice (Fig. 2L and M). Administration of preferential BLT-2 antagonist LY2552833 to Hib infected WT mice had no effect on cellular inflammation or bacterial clearance (Fig. 2L and M), suggesting that BLT-2 is not important in regulating these parameters within this model.

The enzyme 5-lipoxygenase (5-LO) generates leukotriene A_4 (LTA_4), which is subsequently hydrolyzed by LTA_4H into LTB_4 (Supplementary Fig. 3A). To further verify the role of LTB_4 in the outcome of Hib infection we administered the 5-LO inhibitor zileuton to infected animals. Whilst zileuton will inhibit LTB_4 formation, there is the caveat that it could also disrupt production of cysteinyl leukotrienes (LTC_4, D_4, E_4) and lipoxins since they share a common LTA_4 intermediate (Supplementary Fig. 3A). Zileuton administered Hib-infected mice showed comparable cellular inflammation into the airways and lungs at 24hrs (Supplementary Fig. 3B

and C) relative to control treated animals. Furthermore, zileuton administration did not alter neutrophil numbers (Supplementary Fig. 3D and E) but did compromise bacterial clearance (Supplementary Fig. 3F and G).

Hib-infected lta4h-/- mice display augmented inflammation.

Having inferred the role of LTB_4 in Hib infection, it was now of interest to determine the phenotype of Hib-infected lta4h-/- mice that lack the classical pro-inflammatory LTB_4 generating activity but also the anti-inflammatory PGP degrading activity. WT and lta4h-/- mice were infected with $1x10^7$ CFU of Hib and ensuing illness and inflammation assessed. Hib-infected lta4h-/- mice exhibited a more pronounced weight loss that was slower to resolve relative to WT controls (Fig. 3A). In keeping with a more pronounced illness in lta4h-/- mice, they also displayed augmented pulmonary edema (Fig. 3B) and cellular damage (Fig. 3C). The more pronounced illness observed in Hib-infected lta4h-/- mice relative to WT controls was not attributable to compromised bacterial clearance since CFU were comparable in BALF (Fig. 3D) and lung parenchyma (Fig. 3E). Instead, Hib-infected lta4h-/- mice showed a dramatic increase in cellular infiltrate into their airways (Fig. 3F) and lung tissue (Fig. 3G) relative to the WT animals, which was largely attributable to a substantial increase in neutrophils (Fig. 3H and I). Secondary to the augmented neutrophilia seen in lta4h-/- mice was an elevated infiltration of monocytes/macrophages into the airways (Fig. 3J) and lung tissue (Fig. 3K) relative to WT controls.

PGP drives an exacerbated neutrophilic inflammation to Hib.

The augmented neutrophilic inflammation observed in Hib-infected lta4h-/- mice, despite the absence of LTB_4 (Fig. 4A), was not attributable to an elevation in KC and MIP-2 since levels in BALF (Fig. 4B and C) were comparable between WT and lta4h-/- mice. Other neutrophil chemoattractants C5a, lungkine/CXCL15 and ENA-78/CXCL5 were also comparable between WT and lta4h-/- mice (Supplementary Fig. 4A-C). Levels of pro-inflammatory cytokines TNF-α (Fig. 4D) and IL-6 (Fig. 4E), that can regulate neutrophil recruitment, were elevated at 24hrs in Hib-infected lta4h-/- mice but seemed insufficient alone to drive the observed phenotype. However, whilst no PGP was detectable in the BALF of Hib-infected WT mice, significant quantities were present in lta4h-/- animals (Fig. 4F). Accordingly, the capacity of BALF to

degrade PGP was absent in Hib-infected lta4h-/- mice (Fig. 4G and H). PGP administration to Hib-infected WT mice augmented airway neutrophilia (Fig. 4I) and promoted bacterial clearance (Fig. 4J), supporting the notion that the phenotype of the lta4h-/- animals could be attributable to PGP accumulation.

To verify that the exacerbated illness and neutrophilic inflammation observed in lta4h-/- mice was due to PGP accumulation we utilized a complementary peptide that specifically antagonizes PGP, namely Arginine-Threonine-Arginine (RTR)[36, 51]. Hib-infected WT and lta4h-/- mice were administered RTR and inflammation and bacterial burden assessed at 24 hrs post infection. Whilst WT mice again displayed no PGP in their airways, control and RTR-treated lta4h-/- mice exhibited substantial quantities - highlighting that RTR does not reduce levels of PGP but rather binds and antagonizes it (Fig. 4K)[52]. Administration of RTR to Hib-infected lta4h-/- mice completely negated the augmented cellular infiltrate seen in the airways (Fig. 4L) and lungs (Fig. 4M) of these mice above that observed in the WT controls. Furthermore, administration of RTR to lta4h-/- mice compromised bacterial clearance (Fig. 4N) – presumably due to the loss of LTB_4 and now the compensatory PGP that had previously conferred some augmented protection. In keeping with the role of PGP, the reduction in pulmonary inflammation observed in Hib-infected lta4h-/- mice administered RTR was due to a diminished neutrophilic infiltrate (Fig. 4O and P). The previously observed heightened TNF-α and IL-6 release in Hib-infected lta4h-/- mice (Fig. 4D and E) was normalized to WT levels following RTR treatment (Fig. 4Q and R), suggestive that it is secondary to PGP. As a point of note, it has been suggested that loss of LTA_4H function can lead to an accumulation of LTA_4 and a subsequent lipoxin shunt whereby levels of anti-inflammatory lipoxins are increased[53]. If this were the case in Hib-infected lta4h-/- mice then one may envisage a reduced inflammation in response to the bacteria rather than the substantial PGP-driven increase observed. Furthermore, within our model system no lipoxins were detectable at any time point.

Augmented macrophage influx in Hib infected lta4h-/- mice.

PGP is a neutrophil chemoattractant and thus whilst it is rational that a greater neutrophil infiltrate is observed in lta4h-/- mice infected with Hib, it cannot explain the augmented ensuing infiltration of monocytes (Fig. 3J and K). Furthermore, there were comparable levels of classical monocyte-attracting chemokines preceding this monocytic infiltrate in lta4h-/- mice and

littermate controls (Supplementary Fig. 4D-G). Whilst collagen-derived PGP is not chemotactic for monocytes, elastin-derived matrikines are[11, 54, 55]. It was postulated that PGP accumulation in lta4h-/- mice may drive augmented neutrophilic inflammation with ensuing augmented elastase activity, elastin fragment generation and monocyte infiltration; in essence a protease/matrikine driven inflammatory exacerbation.

In keeping with elevated neutrophilic inflammation in Hib-infected lta4h-/- mice there was a significant increase in BALF levels of neutrophil-rich proteases MMP-9 (Fig. 5A) and NE (Fig. 5B). Furthermore, there was an augmentation in MMP-9 mRNA reflective of the substantial influx of neutrophils richly expressing this protease (Fig. 5C). Stimulation of bone marrow neutrophils with PGP elicited the release of MMP-9 and NE (Fig. 5D), demonstrating that the peptide was not only capable of recruiting neutrophils but also driving the secretion of their products. Intriguingly, Hib-infected lta4h-/- mice also displayed elevated macrophage elastase, MMP-12, levels in BALF (Fig. 5E). MMP-12 is predominantly expressed by alveolar macrophages and not neutrophils. There was no difference in MMP-12 mRNA levels between lta4h-/- mice and littermate controls (Fig. 5F) suggestive that increased levels in the BALF of knock out animals was not due to increased expression but rather release from alveolar macrophages..

In keeping with a blunted PGP-driven neutrophilic inflammation in RTR treated lta4h-/- mice, there was a concomitant reduction in BALF MMP-9 (Fig. 5G) and NE levels were trending down ($p=0.1$; Fig. 5H). Furthermore, BALF levels of MMP-12 (Fig. 5I) were reduced, confirming that augmented levels in lta4h-/- animals were secondary to PGP accumulation. NE and MMP-12 can target elastin to generate fragments that are chemotactic for monocytes and could underlie their augmented numbers in Hib infected lta4h-/- mice. To verify this, Hib-infected WT and lta4h-/- mice were treated with BA4 antibody (demonstrated to neutralize chemotactic elastin fragments) and cellular infiltrate assessed at day 4 post infection. BA4 administration to Hib-infected lta4h-/- mice blunted the elevated cellular infiltrate observed in airways (Fig. 5J) and lungs (Fig. 5K) of these animals and was largely attributable to a reduction in numbers of monocytes/macrophages (Fig. 5L and M).

Greater inflammation in S. pneumoniae infected lta4h-/- mice.

To demonstrate that the exacerbated inflammation seen in Hib-infected lta4h-/- mice is not specific to a single model system, we investigated the dual roles of the enzyme following pulmonary infection with the Gram-positive bacteria *Streptococcus pneumoniae*. Infection of 129/S6 mice with *S. pneumoniae* elicited an early weight loss that correlated with size of the inoculating dose of bacteria (Supplementary Fig. 5A). However, unlike with Hib infection, bacterial burden is not efficiently eradicated from the airways or lung tissue (Supplementary Fig. 5 B and C). Coinciding with the early weight loss was a robust inflammation in the airways (Supplementary Fig. 5D) and lung tissue (Supplementary Fig. 5E) that was again predominantly neutrophilic (Supplementary Fig. 5F and G). Key PGP-generating enzymes MMP-9 (Supplementary Fig. 5H) and PE (Supplementary Fig. 5I) were readily induced by *S. pneumoniae* infection but PGP was undetectable at any time point by mass spectrometry. The failure to detect PGP despite the presence of MMP-9/PE was again attributable to extracellular release of LTA_4H and its capacity to degrade PGP (Supplementary Fig. 5J).

WT and lta4h-/- mice were infected with either $1x10^5$ or $1x10^6$ CFU of *S. pneumoniae* and inflammation assessed 24hrs later. Lta4h-/- mice displayed a significant increase in cellular infiltrate into their airways (Supplementary Fig. K) with both doses of bacteria relative to littermate controls, which was largely attributable to a substantial increase in neutrophils (Supplementary Fig. 5L). The augmented neutrophilic infiltrate in *S. pneumoniae*-infected lta4h-/- mice relative to controls was not attributable to compromised bacterial clearance (Supplementary Fig. 5M) but rather to an accumulation of PGP (Supplementary Fig. 5N).

Discussion

LTA_4H is the rate limiting enzyme in LTB_4 biosynthesis, a potent pro-inflammatory mediator implicated in host defense but also an array of pathological conditions. However, we have recently identified a novel anti-inflammatory role for LTA_4H in degrading the neutrophil chemoattractant PGP[19]. The physiological significance of this secondary PGP-degrading activity of LTA_4H has not been addressed, and it is unknown whether a failure to degrade PGP can lead to adverse pathological sequelae despite the absence of LTB_4. To investigate the dual roles of LTA_4H we have primarily utilized an acute lung injury model of *Hib* infection; a model chosen since it evokes a robust pulmonary neutrophilia but both inflammation and infection are readily resolved without complication. In this setting, it is feasible to assess the significance and risks of failing to degrade PGP and infer the importance of both LTA_4H activities in protection and pathology.

Hib infection of WT mice resulted in an acute pulmonary neutrophilia that, together with resident alveolar macrophages, was important for the efficient clearance of bacteria. Concomitant with this early inflammation was induction of the classical intracellular epoxide hydrolase activity of LTA_4H and release of LTB_4, with neutrophils themselves seemingly the prominent source of the LTB_4. Also concurrent with the pulmonary neutrophilic inflammation was an increase in levels of key PGP-generating enzymes MMP-9 and PE. Neutrophils are a prominent source of MMP-9 and PE and are thus capable of generating PGP and promoting their own recruitment and eliciting a vicious cycle of pathology if left unchecked[14, 19, 34-36]. However, despite the robust induction of MMP-9 and PE in response to Hib, no PGP was detectable at any time post infection. This was attributable to the extracellular release of LTA_4H and its potent anti-inflammatory PGP-degrading capacity; thus both LTA_4H activities are operational in our model system. We also report a failure to detect PGP, despite the presence of PGP-generating enzymes, in models of *S. pneumoniae* and influenza infection[19]. We would now argue that PGP degradation by LTA_4H is the norm in settings of acute neutrophilia and instrumental in the efficient resolution of inflammation.

LTA_4H is classically a cytosolic enzyme but in order to perform its PGP-degrading activity it must be released to an extracellular environment. LTA_4H is reported to exhibit wide tissue and

cellular distribution[56], that has been difficult to rationalize since leukocytes are the only cells to express both LTA_4H and 5-LO required for leukotriene biosynthesis. It is feasible that the capacity of LTA_4H to degrade PGP may account for the disproportionate distribution of LTA_4H and 5-LO. We have previously demonstrated epithelial cells and neutrophils to be prominent sources of extracellular LTA_4H[19]. Accordingly, we report a reduction in extracellular LTA_4H in neutrophil depleted Hib-infected mice. Thus neutrophils are capable of both initiating and resolving their own inflammation through the action of LTA_4H, in disparate cellular locations.

Loss of LTB_4 signaling through the use of blt1-/- mice or BLT1 antagonists, or administration of 5-LO inhibitor zileuton, did not alter pulmonary inflammation or illness in response to Hib infection, but significantly compromised bacterial clearance. The reduced capacity to control Hib infection in blt1-/- mice was attributable to reduced phagocytosis and killing of the bacteria on a per cell basis by alveolar macrophages and neutrophils. A clear role for LTB_4 in augmenting phagocytosis and microbicidal activity of macrophages and neutrophils is well established[26, 37-50], with the plethora of studies pertaining to Gram-negative bacteria, *Klebsiella pneumoniae*, particularly pertinent to our studies[26, 37, 39, 44, 45].

Given the potent pro-inflammatory capacity of LTB_4, it seems counterintuitive that there is not a reduced cellular infiltrate in blt1-/- mice or mice administered 5-LO inhibitor zileuton. However, it is interesting to note that reduced neutrophil recruitment to sites of inflammation in 5-LO-/- mice has been observed in some, but certainly not all, experimental models examined[27, 57]. Indeed, a compromised pathogen clearance yet comparable cellular inflammation has been reported previously in mice with a disrupted LTB_4 pathway[26, 42]. Thus it may be that whilst LTB_4 serves an important function in Hib killing on a per cell basis it is not critical for directing cellular inflammation within this model, potentially owing to redundancy with other neutrophil chemoattractants. Alternatively, it is feasible that an absence of LTB_4 signaling reduces cellular inflammation and bacterial clearance and this augmented TLR burden subsequently yields a greater release of conventional neutrophil chemokines that promote further neutrophil recruitment – thus masking the original deficit.

Lta4h-/- mice administered Hib displayed greater illness, which was attributable to an augmented cellular infiltrate and ensuing immunopathological sequelae. Most notable within this phenotype was the striking increase in neutrophilic inflammation of Hib-infected lta4h-/- mice, despite the

loss of LTB_4 and comparable levels of other classical neutrophil chemoattractants. This augmented neutrophilia was attributable to PGP accumulation in lta4h-/- mice, since neutralization of PGP completely ablated neutrophil infiltrate to WT levels. Levels of TNF-α and IL-6, which could regulate neutrophilic inflammation and illness, were also elevated in lta4h-/- mice, but were secondary to PGP accumulation. Thus we show that a failure to degrade PGP has serious implications in the control of neutrophilic inflammation, and that the anti-inflammatory activity of LTA_4H has a clear physiological significance over and above that of its pro-inflammatory action in this setting.

It is perhaps surprising that despite the clear role of LTB_4 in protection against Hib infection, that lta4h-/- mice (which lack LTB_4) displayed a comparable bacterial burden to their littermate controls. However, whilst lta4h-/- mice lack LTB_4, they possess an increase in PGP and ensuing neutrophilic inflammation that seemingly compensates *in vivo*. Neutrophils are critical effector cells within our Hib model and given the capacity of PGP to drive neutrophil recruitment and effector function it is not surprising that PGP can prove protective against bacterial challenge, as highlighted by a previous study[58]. Indeed, we demonstrate that PGP administration to Hib-infected WT mice enhances neutrophilic recruitment and bacterial clearance. Furthermore, we clearly demonstrate that PGP is compensating for the loss of LTB_4 and conferring protection against Hib challenge in lta4h-/- mice, since neutralization of the PGP with RTR restored the compromised bacterial clearance.

PGP can drive MMP-9 release from neutrophils and promote a feed-forward system that generates more PGP and further neutrophil recruitment[59]. Accordingly, we demonstrate that PGP can drive MMP-9 release from neutrophils and observe significantly greater MMP-9 levels in Hib infected lta4h-/- mice – a phenotype that is lost if PGP is neutralized. In addition to MMP-9, we demonstrated Hib-infected lta4h-/- to exhibit a broader protease imbalance with an elevation in NE and MMP-12. The augmented NE is rational given the elevated neutrophil numbers in lta4h-/- mice and the potential of PGP to drive NE from neutrophils. More surprising was the PGP-dependent increase in MMP-12 in Hib-infected lta4h-/- mice. Neutrophils do not produce MMP-12 and it is likely that alveolar macrophages represent the primary source in our Hib model. PGP is unable to directly elicit the release of MMP-12 from alveolar macrophages and one would predict that release results from a neutrophil-alveolar macrophage cross-talk.

Secondary to the elevated neutrophilia and protease imbalance was an augmented monocytic/macrophage infiltrate in the lta4h-/- mice that was seemingly dependent upon elastin-derived matrikines in these mice. Whilst mature, cross-linked elastic fibers are not chemotactic for monocytes, cryptic sequences may be released upon proteolysis by elastolytic enzymes, such as MMP-12 or NE. Such sequences are hydrophobic penta- and hexapeptide repeats such as VGVAPG that has been demonstrated to be chemoctactic for monocytes with optimal activity at approximately 10nM[60-62]. Furthermore, many chemotactic elastin fragments generated *in vivo* are also much larger and thus the combined chemotactic potential of elastin-derived products towards monocytes could be substantial[11]. Therefore, the absence of LTA_4H in response to a fairly innocuous challenge gives rise to an accumulation of PGP and neutrophils and a secondary accumulation of elastin-derived matrikines and macrophage numbers (Supp. fig. 6) – thus two distinct protease-matrikine systems are inherently linked and the implications of a failure to degrade PGP are significant.

Loss of LTA_4H function clearly resulted in an exacerbated PGP-driven pulmonary inflammation and illness in response to Hib infection. However, the importance of the LTA_4H PGP-degrading activity, even over and above the well heralded LTB_4-generating activity, is not unique to Hib infection since we also report a comparable phenotype following challenge with *S. pneumoniae*. Previous interpretation of the role of LTA_4H in neutrophilic inflammation had not considered the unrecognized PGP-degrading secondary activity of LTA_4H and will indeed be complicated by the opposing roles of this bifunctional enzyme. Whilst both 5-LO and LTA_4H knockout mice exhibit reduced inflammation in models of ear inflammation and peritonitis relative to WT mice, the reduction is more pronounced in 5-LO knockouts[63]. It is feasible that deletion of LTA_4H, whilst preventing LTB_4 production, may promote PGP levels giving rise to the intermediary phenotype. Furthermore, in an elastase model of emphysema, lta4h-/- animals exhibited a blunted early neutrophilic response that gave way to elevated numbers at later time points – potentially pointing to disparate temporal roles for the two activities of LTA_4H[64]. The significance of LTA_4H and its dual opposing activities in different instances will be complicated by the availability of enzymes that generate LTA_4 and PGP, the relative intra vs extracellular levels of LTA_4H and many other confounding factors. It is feasible therefore that the relative importance of each of LTA_4H's pathways will be disease and even patient specific.

Whilst we demonstrate the result of PGP accumulation in a system where it is normally degraded, it is worth considering the implications of these studies in the context of the chronic diseases where PGP is not efficiently degraded. PGP is elevated in lung diseases such as COPD and CF, often inversely correlating with disease severity[14-18]. The development of COPD is associated with an accumulation of neutrophils and macrophages and a protease imbalance (specifically MMPs and NE) leading to ECM attack[10-12], and there is accumulating evidence that a protease – matrikine mediated pathology is instrumental in the development of diseases[54]. We have previously demonstrated that cigarette smoke, a key risk factor in the development of COPD, can specifically inhibit the aminopeptidase activity of LTA_4H[18, 19, 65]. In light of our current findings it is likely that the failure of LTA_4H to efficiently degrade PGP is an instrumental and potentially early step in this protease imbalance and augmented neutrophil and macrophage infiltrate. It is also noteworthy that *H. influenzae* and *S. pneumoniae* are common exacerbators of COPD and that PGP and neutrophils/proteases have been demonstrated to spike with exacerbations[17, 66, 67]. One can thus envisage a scenario whereby such a bacterial challenge leads to further PGP generation in a setting whereby the peptide cannot be degraded. Targeting the PGP pathway may therefore offer therapeutic potential in chronic neutrophilic lung diseases characterized by PGP accumulation, and in infectious exacerbations of these diseases[28, 68,69, 70].

It is important to question the significance of these findings in the context of therapeutic strategies that seek to inhibit LTA_4H to reduce LTB_4-mediated pathologies[29]. There has been a significant pharmaceutical effort to generate LTA_4H inhibitors but despite the development of drugs that show excellent pharmacokinetic profiles none of these compounds have shown efficacy in clinical trials. These inhibitors seem unlikely to distinguish between the opposing activities of LTA_4H and may therefore inadvertently prevent PGP degradation with adverse effects.

In conclusion, we show for the first time the consequences of a failure to degrade PGP, highlighting a critical role for the secondary anti-inflammatory activity of LTA_4H. In response to a relatively innocuous pulmonary challenge, accumulation of PGP leads to an augmented neutrophilic inflammation and ensuing illness as well as a general protease imbalance that targets the ECM and further perpetuates inflammation. These studies have significant implications for our basic understanding of LTA_4H biology, the cross talk between protease-matrikine networks,

the role of PGP in the pathology and development of chronic lung diseases and the design and application of LTA_4H inhibitors by pharmaceutical companies.

Materials and Methods

Haemophilus influenzae b

Hib Eagan strain was a kind gift from Professor T. Hussell (Institute of Inflammation and Repair, The University of Manchester, UK). Bacteria were cultured at 37°C in 5% CO_2 in Brain heart Infusion (BHI) broth (OXOID, Hampshire, UK) supplemented with 10μg/ml of both Hemin (Roche, West Sussex, UK) and Nictinamide adenine dinucleotide (NAD) (Sigma-Aldrich, Dorset, UK) or on BHI agar (OXOID, Hampshire, UK) supplemented with 4 % Levinthals. Levinthals was made by adding 50 % horse blood (TCS Biosciences, Buckingham, UK) to BHI broth and heating to 70°C for 45 minutes. On cooling to 50°C, 0.7 mg/ml NAD was added and the supernatant stored at -80°C. Bacteria were cultured to an OD600 of 0.3 (approximately 1 x 10^9 CFU/ml) and stored at -80°C in 10 % glycerol as single use aliquots.

Streptococcus pneumoniae

S. pneumoniae (serotype 2) strain D39 (NCTC 7466, National Collection of Type Cultures, London, UK), a kind gift from Professor T. Hussell (Institute of Inflammation and Repair, The University of Manchester, UK) was cultured at 37°C in 5% CO_2 on blood agar plates or in Todd-Hewitt broth (OXOID) supplemented with 0.5 % yeast extract (OXOID, UK) (THY broth) to an OD600 of 0.4 (approximately 1 x 10^8 CFU/ ml) and stored at -80 °C in 10 % glycerol as single use aliquots.

Mice

Six- to eight-week-old female BALB/c and C57BL/6 mice were purchased from Harlan Olac Ltd (Oxon, UK). *Blt1*$^{-/-}$, on a C57BL/6 background, were purchased from Jackson Labs (Bar Harbor, ME), and *Lta4h*$^{-/-}$ mice and littermate controls were on a 129/S6 background and a gift from Dr Y.M. Shim (University of Virginia, Charlottesville, VA). All WT 129/S6 mice referred to within the manuscript are littermate controls of lta4h-/- mice. All mice were kept in specified-pathogen-free conditions and provided autoclaved food, water and bedding. This study was carried out in accordance with the recommendations in the Guide for the Use of Laboratory Animals of Imperial College London. All animal procedures and care conformed strictly to the UK Home Office Guidelines under the Animals (Scientific Procedures) Act 1986, and the protocols were approved by the Home Office of Great Britain.

Lta4h$^{-/-}$ and *Blt1-/-* mice were genotyped by PCR on genomic DNA extracted using the Extract-N-Amp Tissue PCR Kit (Sigma-Aldrich, Dorset, UK). The wild type expression of LTA_4H was detected by primers oIMR1720 (5->3: CGA ATC CAT GCT TAA AAT TGC) and oIMR1721 (5->3: GCG TTA CGA ACG TGA GAC AA) to yield a product size of 128 bp, and *Lta4h*$^{-/-}$ LTA_4H was detected by primers oIMR6916 (5->3: CTT GGG TGG AGA GGC TAT TC) & oIMR6917 (5->3: AGG TGA GAT GAC AGG AGA TC) to yield a product size of 280 bp. Amplification was achieved by PCR (94°C for 3 min > 35 x 2.5min cycles (30 sec at 94°C > 60 sec at 60°C > 60 sec at 72°C) > 72°C for 2 min). The BLT1 expression was detected by primers oIMR8160 (5->3: ATA GCT TTG TAG TGT GGA GCA TCC TGA), oIMR8161 (5->3: TGG AAG ACT TTA TGC TCT TTG TTG GGA) and oIMR8162 (5->3: TGG ATG TGG AAT GTG TGC GAG) to yield a product size of 433 bp for wild type and 270 bp for mutant. Amplification was achieved by PCR (94°C for 3 min > 35 x 2.5min cycles (30 sec at 94°C > 60 sec at 64°C > 60 sec at 72°C) > 72°C for 2 min). Amplification fragments were visualized on 2% agarose gels.

Mouse infection model

Mice were anaesthetized with isoflourane and infected intranasally (i.n.) with 1 x 10^6 or 1 x 10^7 CFU Hib or with 1 x 10^5 or 1 x 10^6 CFU *S. pneumoniae* in 50µl of sterile PBS. Mice were monitored daily and weight loss recorded. In neutrophil depletion experiments, 129/S6 mice received intraperitoneal (i.p.) administration of 500µg and i.n. administration of 200µg of anti-Ly6G (1A8, Bio X Cell, West Lebanon, NH), or control rat IgG (2A3, Bio X Cell, West Lebanon, NH) the day preceding and the day of infection and culled 24 hours later. In alveolar macrophage depletion experiments, 129/S6 mice received i.n. administration of 50 µl of control or clodronate liposomes (ClodronateLiposomes.com) 24hrs and 48hrs prior to infection and culled 24 hours post infection. In some experiments, BLT-1 specific antagonist U-75302 (Cayman Chemical Company, Ann Arbor, MI) or BLT-2 specific antagonist LY2552833 (Cayman Chemical Company, Ann Arbor, MI) or vehicle controls were administered at a dose of 100µg i.p. to 129/S6 mice 1 hour prior to infection and 9 hours post infection before being culled at 24 hrs post infection. In some experiments mice were each intraperitoneally administered 500µg of zileuton (Sigma-Aldrich, Dorset, UK) the day preceding and the day of infection and culled 24 hrs later. Zileuton was dissolved in a 50% solution of DMSO (Sigma-Aldrich, Dorset, UK) in saline, with a final volume of 100µL. A similar volume of DMSO was given intraperitoneally to control mice in these experiments. In some experiments, mice were

administered i.n. 250µg AcPGP (BACHEM, Bubendorf, Switzerland) or control AcPGG (BACHEM, Bubendorf, Switzerland) peptide 2 hrs post infection and culled at 24 hrs. To neutralize PGP, mice were administered Arginine-Threonine-Arginine (RTR) peptide (Anaspec peptides, Fremont, CA) at a dose of 100µg i.n. to mice 1 and 9 hours post infection before being culled at 24 hrs. To neutralize elastin fragments, mice were administered BA4 (Sigma-Aldrich, Dorset, UK) or control antibody at a dose of 50µg i.n. to mice on a daily basis from time of infection before being culled at day 4.

Cell recovery and isolation

Mice were administered 3 mg pentobarbital and exsanguinated via the femoral artery. Serum was isolated by centrifugation for 8 min at 5000xg and frozen at –80°C until required. The lungs were then inflated 5 times with 1.5ml PBS via an intratracheal cannula and 100µl from each mouse removed for enumeration of bacterial burden (see below). The remainder was centrifuged and the supernatant stored at –80°C. The pellet was resuspended at 10^6 cells / ml in R10F (RPMI containing 10% (vol/vol) FCS, penicillin (50U/ml), streptomycin (50µg/ml) and L-glutamine (2mM)) and cell viability was assessed using trypan blue exclusion. Lung tissue was disrupted to a single cell suspension by passage through a 100µM sieve (BD labware, New Jersey). 100µl from each mouse was again removed for enumeration of bacterial burden and the remaining cell suspension was centrifuged for 5 min at 800xg and red blood cells lysed by resuspending pellets in ACK buffer (0.15M ammonium chloride, 1M potassium hydrogen carbonate and 0.01mM EDTA, pH 7.2) for 3 minutes at room temperature before centrifugation (800xg for 5 min) and resuspending in R10F. Cell viability was assessed by trypan blue exclusion and cells resuspended in R10F at 10^6 cells/ml.

Alveolar macrophages were isolated by adherence of BAL fluid to plastic for 1h in DMEM at 37°C, 5% CO_2 and shown to be >97% pure by flow cytometric analysis. To isolate bone marrow neutrophils, the femur and the tibia from both hind legs were removed and freed of soft tissue attachments, and the extreme distal tip of each extremity cut off. HBSS containing 15mM EDTA and 30mM HEPES was forced through the bone with a syringe. After dispersing cell clumps and passage through a 100µM sieve (BD labware, New Jersey), red blood cells were lysed by resuspending pellets in ACK buffer (for 3 minutes at room temperature) before centrifugation (800xg 5 min) and washing with HBSS. The cell suspension was centrifuged (800xg, 5 min, 4°C)

and resuspended in RPMI. The cells were layered onto a 72%, 64%, 52% Percoll gradient (Sigma-Aldrich, UK) diluted in PBS (100% Percoll = nine parts Percoll and one part 10x PBS), and centrifuged (1500xg, 30 min, room temperature) without braking. The neutrophils at the 64%/72% interface were harvested and washed with 20 ml RPMI. Cell viability was assessed by trypan blue exclusion and confirmed to be > 90% neutrophils by flow cytometry.

Bacterial CFU enumeration

BALF and lung suspension (as detailed above) were serially diluted in sterile PBS and plated on to appropriate agar plates (Columbia blood agar plates for *S. pneumoniae*, BHI agar with 4 % Levinthals for Hib) and grown overnight at 37 °C with 5% CO_2. Resultant colonies were counted manually. *S. pneumoniae* was confirmed by optochin sensitivity. Hib was confirmed by no growth on BHI agar without Levinthals.

Flow cytometry

Single-cell suspensions were stained for surface markers in PBS containing 0.1% sodium azide and 1% BSA for 30 min at 4 °C and fixed with 2% paraformaldehyde. Data was acquired on a BD FACS Fortessa machine (BD Biosystems, UK). Forward scatter and side scatter gates were used to exclude debris and dead cells were excluded using a fixable near IR dead cell stain kit for 633 or 635 nm excitation. Cell types were characterized by their forward and side scatter profiles and by their phenotypes:

Cell Type	Surface Marker Phenotype	Monoclonal Antibody Conjugate	Catalogue Number	Dilution
B Cells	$CD19^+$	CD19-FITC (BD Biosciences)	557398	1/100
	$CD3^-$	CD3-PECy7 (eBioscience)	25-0031	1/200
Natural Killer (NK) Cells	$NKp46^+$	NKp46-PE (eBioscience)	12-3351	1/200
	$CD3^-$	CD3-PECy7 (eBioscience)	25-0031	1/200
$CD4^+$ T Cells	$CD4^+$	CD4-PerCP (BD Biosciences)	553052	1/200
	$CD3^+$	CD3-PECy7 (eBioscience)	25-0031	1/200
$CD8^+$ T Cells	$CD8^+$	CD8-APC (BD Biosciences)	553035	1/200
	$CD3^+$	CD3-PECy7 (eBioscience)	25-0031	1/200
Neutrophils	$Ly\text{-}6G^{high}$	Ly6G-FITC (BD Biosciences)	551460	1/100
	$CD11b^{high}$	CD11b-PerCP (eBioscience)	45-0112	1/400
	$CD11c^{low}$	CD11c-APC (BD Biosciences)	550261	1/200
	$F4/80^{low}$	F4/80-PE (eBioscience)	12-4801	1/50
Alveolar Macrophages	$CD11b^{low\text{-}int.}$	CD11b-PerCP (eBioscience)	45-0112	1/400
	$CD11c^{high}$	CD11c-APC (BD Biosciences)	550261	1/200
	$F4/80^{high}$	F4/80-PE (eBioscience)	12-4801	1/50
Inflammatory monocytes/ macrophages	$CD11b^{high}$	CD11b-PerCP (eBioscience)	45-0112	1/400
	$CD11c^{low}$	CD11c-APC (BD Biosciences)	550261	1/200
	$F4/80^{high}$	F4/80-PE (eBioscience)	12-4801	1/50

Table 1. Characterization of immune cells by flow cytometry.

Treatment of neutrophils with Ac-PGP

Pre-warmed neutrophil suspensions (37°C, 2×10^6 cells/ml) were incubated in 1% BSA/HBSS with or without AcPGP (0.1mg/ml; BACHEM, Bubendorf, Switzerland) or IL-8 (1µg/ml) for 15 min at 37°C in 5% CO_2. The level of enzymes released in cell-free supernatant was measured by ELISA-based assays (see below).

Alveolar macrophage and neutrophil phagocytsosis assay

Alveolar macrophages (pre-adhered; $1x10^5$) or bone marrow derived neutrophils (in suspension; $1x10^5$) from WT and blt1-/- mice were incubated with *Haemophilus influenzae* b (MOI 20:1; with 10% serum) conjugated with pHrodo dye utilizing the pHrodo Phagocytosis Particle Labeling Kit (Invitrogen, USA) and phagocytosis assessed by flow cytometry according the manufacturer's directions. pHrodo is a fluorogenic dye that exhibits low fluorescence at neutral pH but fluoresces in acidic environments, allowing accurate measurement of the engulfment of pHrodo-labelled bacteria into the acidic phagosome.

Alveolar macrophage and neutrophil killing assay

Alveolar macrophages (pre-adhered; $5x10^5$) or bone marrow derived neutrophils (in suspension; $1x10^6$) from WT and blt1-/- mice were infected with *Haemophilus influenzae* b (MOI 1:1) in RPMI with 5% serum at 37°C. After 15 min extracellular bacteria were removed by washing 3x with ice cold RPMI and cells were resuspended in 300µl RPMI/5% serum and incubated at 37°C. At 0, 30 and 60 min 100µl samples were removed and diluted into 900µl H_2O. Cells were allowed to lyse by standing at room temperature for 10 min and were subsequently vortexed vigorously to disperse bacteria. Samples were further diluted in H_2O, plated on BHI agar with 4 % Levinthals and grown overnight at 37°C with 5% CO_2. Resultant colonies were counted and % original CFU burden determined relative to the t = 0 min time point.

Protease quantification and activity

The concentration of MMP-9 in BALF and neutrophil supernatants was measured using an ELISA, according to the manufacturer's directions (R&D Systems, Minneapolis, MN). To assess MMP-9 gelatinolytic activity, BALF was mixed 1:1 (vol:vol) with Tris-Glycine-SDS Sample Buffer (Life Technologies Ltd, Paisley, UK) and loaded onto 10% zymogram (gelatin) gels (Life Technologies Ltd, Paisley, UK). Samples were subsequently electrophoresed at 125 V for 90 minutes in Tris-Glycine-SDS Running Buffer (Life Technologies Ltd, Paisley, UK). Following electrophoresis, gels were incubated in 1X Zymogram Renaturing Buffer (Life Technologies Ltd, Paisley, UK) for 30 minutes at room temperatrue. To visualize the gelatinolytic activity, the gel was incubated in 1X Zymogram Developing Buffer (Life Technologies Ltd, Paisley, UK) overnight at 37˚C before staining with SimplyBlue™ Safestain (Life Technologies Ltd, Paisley, UK).

The concentrations of LTA_4H, NE and MMP-12 in BALF and/or neutrophil supernatants were measured using an ELISA, according to the manufacturer's directions (USCN Life Science, Hubei, PRC).

PE activity assay

20µl of BALF was incubated with a specific substrate (2 mM Benzylcarboxy-Glycine-Proline-para-Nitroaniline, ZGP-pNa; Chem-Impex, Wood Dale, IL) at 37^{o}C and 5% CO_2 and cleavage of para-nitroaniline (pNa) from the substrate by PE was detected using a spectrophotometer at 410 nm.

ESI-LC/MS/MS for PGP detection

For peptide quantification in BALF, PGP and AcPGP were measured using a MDS Sciex (Applied Biosystems, Foster City, CA) API-4000 spectrometer equipped with a Shimadzu HPLC (Columbia, MD). For peptide quantification from degradation experiments, PGP and AcPGP were measured using a Thermo Accela Pump and Autosampler coupled to a Thermo TSQ Quantum Access. HPLC was done using a 2.0 x 150 mm Jupiter 4u Proteo column (Phenomenex, Torrance, CA) with A: 0.1% HCOOH and B: MeCN + 0.1% HCOOH: 0 min-0.5 min 5% buffer B/95% buffer A, then increased over 0.5-2.5 min to 100% buffer B/0% buffer A. Background was removed by flushing with 100% isopropanol / 0.1% formic acid. Positive electrospray mass transitions were at 270-70, 270-116 and 270-173 for PGP and 312-140 and 312-112 of AcPGP.

PGP degradation experiments

Bronchoalveolar lavage fluid (diluted 1/10 in PBS) was incubated with 0.4mM PGP at 37^{o}C and 5% CO_2 for 2 hrs. Concentrations of PGP remaining were subsequently quantified by ESI-LC/MS/MS (as discussed above) by comparison with PGP standards. The percentage of peptide degraded was determined relative to control samples of 0.4mM PGP alone.

Measurement of free proline

Aliquots from PGP degradation experiments were diluted 1 in 10 in PBS (to a final volume of 250µl). Glacial acetic acid (250µl) was then added, followed by 250µl of ninhydrin solution (25 mg/ml in acetic acid/6 M phosphoric acid; heated at 70°C to dissolve). The reaction mixture

was heated at 100°C for 60 minutes, allowed to cool to room temperature and the proline containing fraction extracted with 500µl of toluene and optical density measured at 520 nm.

LTA_4H epoxide hydrolase activity

50µl of the BAL cell suspension was added to 50µl of RPMI and treated with A23187 at a final concentration of 2µg/ml. 1% DMSO was used as a control. Cells were incubated for 20 minutes at 37˚C, and supernatants removed and stored at -80˚C for subsequent LTB_4 analysis (as described below).

LTB_4 quantification

The actual concentration of LTB_4 in the BALF and that generated in the epoxide hydrolase activity assay (above) was assayed using an ELISA, according to manufacturer's directions (R&D systems, Minneapolis, MN) or for maximal sensitivity/specificity using a MDS Sciex (Applied Biosystems, Foster City, CA) API-4000 spectrometer equipped with a Shimadzu HPLC (Columbia, MD). HPLC was done using a 2.1 x 100 mm Kinetex column (Phenomenex, Torrance, CA) with A: 10 mM NH_4OAc and B: MeCN + 10 mM NH_4OAc: 0 min-0.5 min 5% buffer B/95% buffer A, then increased over 0.5-5 min to 100% buffer B/0% buffer A. Negative electrospray mass transitions were at 335-195, 335-151 and 335-123 for LTB_4.

Cytokine / chemokine quantification

The levels of CXCL1/KC, CXCL2/MIP-2, MCP-1/CCL2, C5a, Lungkine/CXCL15, TNF-α, IL-6 (Duo Set; R&D Systems, Minneapolis, MN) and MCP-3/CCL7 (MyBiosource, San Diego, CA) were measured according to the manufacturer's instructions.

Albumin ELISA

The concentration of albumin in BALF was measured using an ELISA, according to the manufacturer's directions (Bethyl Laboratories, Montgomery, TX).

Lactate dehydrogenase (LDH) assay

LDH activity in BALF was assessed using the Lactate Dehydrogenase Activity Assay Kit (Sigma-Aldrich, Dorset, UK). Equal volumes of LDH substrate, LDH assay dye and LDH assay

cofactor preparation were combined and 100µl was added to 50µl of sample. The samples were incubated at room temperature in the dark for 30 minutes. The reaction was stopped using 30µl 1N HCl and absorbance determined using a spectrophotometer (490 nm).

Real-time PCR

Total RNA was extracted from 50 to 100 mg of lung tissue (azygous lobe) using a Qiagen RNeasy Mini Kit. Total RNA (1µg) was reverse transcribed into cDNA using a High Capacity cDNA Reverse Transcription Kit (Life Technologies) as per the manufacturer's instructions. Real-time PCR reactions were performed using fast-qPCR mastermix (Life technologies) on a Viaa-7 instrument (Life Technologies) with TaqMan primer sets for murine ENA-78/CXCL5, MCP-1/CCL2, MCP-3/CCL7, MMP-9, MMP-12, GAPDH or HPRT (Life Technologies) and gene expression was analyzed using the change-in-threshold ΔΔCt- method, fold-changes in mRNA expression for targeted genes were calculated relative to naïve wild-type controls.

Statistical analysis

Statistical significance was calculated using an unpaired Mann-Whitney test. All p-values of ≤ 0.05 (*) and ≤ 0.01(**) were considered significant and are referred to as such in the text.

Author Contributions

RJS planned, executed and interpreted the experiments and prepared the manuscript; SA did many experiments and assisted with the analysis; RCB, DFP, TPS and XX provided technical contributions to the paper; PLJ aided with mass spectrometry, and AG, PLJ, JEB and CML contributed discussions throughout the work.

Acknowledgements

RJS is a Wellcome Trust Career Development Fellow (095707/Z/11/Z). CML is a Wellcome Trust Senior Fellow in Basic Biomedical Sciences (086718/Z/08/Z). TP is supported by a Marie Curie Intra European Fellowship within the 7th European Community Framework Programme (FP7-PEOPLE-2013-IEF N°627374). The National Heart, Lung and Blood Institute funds JEB (HL07783, HL110950 and HL114439) and AG (HL102371-A1). The UAB Lung Health Center

Pulmonary Proteomics Laboratory is funded through the NIH (RR19231, P30CA13148, P50AT00277, U54CA100949, P30AR050948 and P30DK740380). We would like to thank Dr Anna Caldwell and the Centre of Excellence for Mass Spectrometry at King's College London for the use of equipment and technical assistance.

Conflict of Interest

The authors have no conflict of interest.

References

1. Reeves, E.P. *et al.* Killing activity of neutrophils is mediated through activation of proteases by K+ flux. *Nature* **416**, 291-297 (2002).
2. Stuart, L.M. & Ezekowitz, R.A. Phagocytosis: elegant complexity. *Immunity* **22**, 539-550 (2005).
3. Rot, A. & von Andrian, U.H. Chemokines in innate and adaptive host defense: basic chemokinese grammar for immune cells. *Annu Rev Immunol* **22**, 891-928 (2004).
4. Nathan, C. Neutrophils and immunity: challenges and opportunities. *Nat Rev Immunol* **6**, 173-182 (2006).
5. Mantovani, A., Cassatella, M.A., Costantini, C. & Jaillon, S. Neutrophils in the activation and regulation of innate and adaptive immunity. *Nat Rev Immunol* **11**, 519-531 (2011).
6. O'Donnell, R., Breen, D., Wilson, S. & Djukanovic, R. Inflammatory cells in the airways in COPD. *Thorax* **61**, 448-454 (2006).
7. Rowe, S.M., Miller, S. & Sorscher, E.J. Cystic fibrosis. *N Engl J Med* **352**, 1992-2001 (2005).
8. Djekic, U.V., Gaggar, A. & Weathington, N.M. Attacking the multi-tiered proteolytic pathology of COPD: new insights from basic and translational studies. *Pharmacol Ther* **121**, 132-146 (2009).
9. Shapiro, S.D. *et al.* Neutrophil elastase contributes to cigarette smoke-induced emphysema in mice. *Am J Pathol* **163**, 2329-2335 (2003).
10. Churg, A. *et al.* Acute cigarette smoke-induced connective tissue breakdown requires both neutrophils and macrophage metalloelastase in mice. *Am J Respir Cell Mol Biol* **27**, 368-374 (2002).
11. Houghton, A.M. *et al.* Elastin fragments drive disease progression in a murine model of emphysema. *J Clin Invest* **116**, 753-759 (2006).
12. Hautamaki, R.D., Kobayashi, D.K., Senior, R.M. & Shapiro, S.D. Requirement for macrophage elastase for cigarette smoke-induced emphysema in mice. *Science* **277**, 2002-2004 (1997).
13. Weathington, N.M. *et al.* A novel peptide CXCR ligand derived from extracellular matrix degradation during airway inflammation. *Nat Med* **12**, 317-323 (2006).
14. Gaggar, A. *et al.* A novel proteolytic cascade generates an extracellular matrix-derived chemoattractant in chronic neutrophilic inflammation. *J Immunol* **180**, 5662-5669 (2008).
15. Hardison, M.T. *et al.* The presence of a matrix-derived neutrophil chemoattractant in bronchiolitis obliterans syndrome after lung transplantation. *J Immunol* **182**, 4423-4431 (2009).
16. O'Reilly, P. *et al.* N-alpha-PGP and PGP, potential biomarkers and therapeutic targets for COPD. *Respir Res* **10**:38 (2009).
17. O'Reilly, P.J. *et al.* Sputum PGP is reduced by azithromycin treatment in patients with COPD and correlates with exacerbations. *BMJ Open* **3**, e004140 (2013).
18. Wells, J.M. *et al.* An aberrant leukotriene A4 hydrolase-proline-glycine-proline pathway in the pathogenesis of chronic obstructive pulmonary disease. *Am J Respir Crit Care Med* **190**, 51-61 (2014).
19. Snelgrove, R.J. *et al.* A critical role for LTA4H in limiting chronic pulmonary neutrophilic inflammation. *Science* **330**, 90-94 (2010).
20. Haeggstrom, J.Z., Tholander, F. & Wetterholm, A. Structure and catalytic mechanisms of leukotriene A4 hydrolase. *Prostaglandins Other Lipid Mediat* **83**, 198-202 (2007).
21. Funk, C.D. Prostaglandins and leukotrienes: advances in eicosanoid biology. *Science* **294**, 1871-1875 (2001).
22. Tager, A.M. & Luster, A.D. BLT1 and BLT2: the leukotriene B(4) receptors. *Prostaglandins Leukot Essent Fatty Acids* **69**, 123-134 (2003).

23. Di Gennaro, A. & Haeggstrom, J.Z. The leukotrienes: immune-modulating lipid mediators of disease. *Adv Immunol* **116**, 51-92 (2012).
24. Whittle, B.J. *et al.* Attenuation of inflammation and cytokine production in rat colitis by a novel selective inhibitor of leukotriene A4 hydrolase. *Br J Pharmacol* **153**, 983-991 (2008).
25. Griffiths, R.J. *et al.* Leukotriene B4 plays a critical role in the progression of collagen-induced arthritis. *Proc Natl Acad Sci U S A* **92**, 517-521 (1995).
26. Bailie, M.B. *et al.* Leukotriene-deficient mice manifest enhanced lethality from Klebsiella pneumonia in association with decreased alveolar macrophage phagocytic and bactericidal activities. *J Immunol* **157**, 5221-5224 (1996).
27. Chen, X.S., Sheller, J.R., Johnson, E.N. & Funk, C.D. Role of leukotrienes revealed by targeted disruption of the 5-lipoxygenase gene. *Nature* **372**, 179-182 (1994).
28. Snelgrove, R.J. Leukotriene A4 hydrolase: an anti-inflammatory role for a proinflammatory enzyme. *Thorax* **66**, 550-1 (2011).
29. Fourie, A.M. Modulation of inflammatory disease by inhibitors of leukotriene A4 hydrolase. *Curr Opin Investig Drugs* **10**, 1173-1182 (2009).
30. Barchuk, W. *et al.* Effects of JNJ-40929837, a leukotriene A4 hydrolase inhibitor, in a bronchial allergen challenge model of asthma. *Pulm Pharmacol Ther* **29**, 15-23 (2014).
31. Ulanova, M. & Tsang, R.S. Invasive Haemophilus influenzae disease: changing epidemiology and host-parasite interactions in the 21st century. *Infect Genet Evol* **9**, 594-605 (2009).
32. Ulanova, M. & Tsang, R.S. Haemophilus influenzae serotype a as a cause of serious invasive infections. *Lancet Infect Dis* **14**, 70-82 (2014).
33. Kelly, D.F., Moxon, E.R. & Pollard, A.J. Haemophilus influenzae type b conjugate vaccines. *Immunology* **113**, 163-174 (2004).
34. O'Reilly, P.J. *et al.* Neutrophils contain prolyl endopeptidase and generate the chemotactic peptide, PGP, from collagen. *J Neuroimmunol* **217**, 51-54 (2009).
35. Overbeek, S.A. *et al.* Cigarette smoke-induced collagen destruction; key to chronic neutrophilic airway inflammation? *PLoS One* **8**, e55612 (2013).
36. Braber, S. *et al.* Cigarette smoke-induced lung emphysema in mice is associated with prolyl endopeptidase, an enzyme involved in collagen breakdown. *Am J Physiol Lung Cell Mol Physiol* **300**, L255-265 (2010).
37. Serezani, C.H., Aronoff, D.M., Jancar, S., Mancuso, P. & Peters-Golden, M. Leukotrienes enhance the bactericidal activity of alveolar macrophages against Klebsiella pneumoniae through the activation of NADPH oxidase. *Blood* **106**, 1067-1075 (2005).
38. Soares, E.M. *et al.* Leukotriene B4 enhances innate immune defense against the puerperal sepsis agent Streptococcus pyogenes. *J Immunol* **190**, 1614-1622 (2013).
39. Mancuso, P., Nana-Sinkam, P. & Peters-Golden, M. Leukotriene B4 augments neutrophil phagocytosis of Klebsiella pneumoniae. *Infect Immun* **69**, 2011-2016 (2001).
40. Mancuso, P., Lewis, C., Serezani, C.H., Goel, D. & Peters-Golden, M. Intrapulmonary administration of leukotriene B4 enhances pulmonary host defense against pneumococcal pneumonia. *Infect Immun* **78**, 2264-2271 (2010).
41. Serezani, C.H., Perrela, J.H., Russo, M., Peters-Golden, M. & Jancar, S. Leukotrienes are essential for the control of Leishmania amazonensis infection and contribute to strain variation in susceptibility. *J Immunol* **177**, 3201-3208 (2006).
42. Peres, C.M. *et al.* Inhibition of leukotriene biosynthesis abrogates the host control of Mycobacterium tuberculosis. *Microbes Infect* **9**, 483-489 (2007).
43. Wirth, J.J. & Kierszenbaum, F. Stimulatory effects of leukotriene B4 on macrophage association with and intracellular destruction of Trypanosoma cruzi. *J Immunol* **134**, 1989-1993 (1985).

44. Mancuso, P., Standiford, T.J., Marshall, T. & Peters-Golden, M. 5-Lipoxygenase reaction products modulate alveolar macrophage phagocytosis of Klebsiella pneumoniae. *Infect Immun* **66**, 5140-5146 (1998).
45. Mancuso, P. & Peters-Golden, M. Modulation of alveolar macrophage phagocytosis by leukotrienes is Fc receptor-mediated and protein kinase C-dependent. *Am J Respir Cell Mol Biol* **23**, 727-733 (2000).
46. Demitsu, T., Katayama, H., Saito-Taki, T., Yaoita, H. & Nakano, M. Phagocytosis and bactericidal action of mouse peritoneal macrophages treated with leukotriene B4. *Int J Immunopharmacol* **11**, 801-808 (1989).
47. Talvani, A. *et al.* Leukotriene B(4) induces nitric oxide synthesis in Trypanosoma cruzi-infected murine macrophages and mediates resistance to infection. *Infect Immun* **70**, 4247-4253 (2002).
48. Coffey, M.J., Phare, S.M. & Peters-Golden, M. Role of leukotrienes in killing of Mycobacterium bovis by neutrophils. *Prostaglandins Leukot Essent Fatty Acids* **71**, 185-190 (2004).
49. Larfars, G., Lantoine, F., Devynck, M.A., Palmblad, J. & Gyllenhammar, H. Activation of nitric oxide release and oxidative metabolism by leukotrienes B4, C4, and D4 in human polymorphonuclear leukocytes. *Blood* **93**, 1399-1405 (1999).
50. Ito, N. *et al.* Requirement of phosphatidylinositol 3-kinase activation and calcium influx for leukotriene B4-induced enzyme release. *J Biol Chem* **277**, 44898-44904 (2002).
51. van Houwelingen, A.H. *et al.* Induction of lung emphysema is prevented by L-arginine-threonine-arginine. *FASEB J* **22**, 3403-3408 (2008).
52. Pfister, R.R. *et al.* Synthetic complementary peptides inhibit a neutrophil chemoattractant found in the alkali-injured cornea. *Cornea* **19**, 384-389 (2000).
53. Rao, N.L. *et al.* Anti-inflammatory activity of a potent, selective leukotriene A4 hydrolase inhibitor in comparison with the 5-lipoxygenase inhibitor zileuton. *J Pharmacol Exp Ther* **321**, 1154-1160 (2007).
54. He, J., Turino, G.M. & Lin, Y.Y. Characterization of peptide fragments from lung elastin degradation in chronic obstructive pulmonary disease. *Exp Lung Res* **36**, 548-557 (2013).
55. Blanchevoye, C. *et al.* Interaction between the elastin peptide VGVAPG and human elastin binding protein. *J Biol Chem* **288**, 1317-1328 (2013).
56. Haeggstrom, J.Z. Structure, function, and regulation of leukotriene A4 hydrolase. *Am J Respir Crit Care Med* **161**, S25-31 (2000).
57. Goulet, J.L., Snouwaert, J.N., Latour, A.M., Coffman, T.M. & Koller, B.H. Altered inflammatory responses in leukotriene-deficient mice. *Proc Natl Acad Sci U S A* **91**, 12852-12856 (1994).
58. Kim, S.D. *et al.* Activation of CXCR2 by Extracellular Matrix Degradation Product Acetylated-Pro-Gly-Pro has Therapeutic Effects Against Sepsis. *Am J Respir Crit Care Med* **184**, 243-51 (2011).
59. Xu, X. *et al.* A self-propagating matrix metalloprotease-9 (MMP-9) dependent cycle of chronic neutrophilic inflammation. *PLoS One* **6**, e15781 (2011).
60. Senior, R.M., Griffin, G.L. & Mecham, R.P. Chemotactic activity of elastin-derived peptides. *J Clin Invest* **66**, 859-862 (1980).
61. Senior, R.M. *et al.* Val-Gly-Val-Ala-Pro-Gly, a repeating peptide in elastin, is chemotactic for fibroblasts and monocytes. *J Cell Biol* **99**, 870-874 (1984).
62. Hunninghake, G.W. *et al.* Elastin fragments attract macrophage precursors to diseased sites in pulmonary emphysema. *Science* **212**, 925-927 (1981).
63. Byrum, R.S., Goulet, J.L., Snouwaert, J.N., Griffiths, R.J. & Koller, B.H. Determination of the contribution of cysteinyl leukotrienes and leukotriene B4 in acute inflammatory responses using 5-lipoxygenase- and leukotriene A4 hydrolase-deficient mice. *J Immunol* **163**, 6810-6819 (1999).
64. Shim, Y.M. *et al.* Role of LTB(4) in the pathogenesis of elastase-induced murine pulmonary emphysema. *Am J Physiol Lung Cell Mol Physiol* **299**, L749-759 (2010).

65. Hardison, M.T., Brown, M.D., Snelgrove, R.J., Blalock, J.E. & Jackson, P. Cigarette smoke enhances chemotaxis via acetylation of proline-glycine-proline. *Front Biosci (Elite Ed)* **4**, 2402-2409 (2012).
66. Wedzicha, J.A., Brill, S.E., Allinson, J.P. & Donaldson, G.C. Mechanisms and impact of the frequent exacerbator phenotype in chronic obstructive pulmonary disease. *BMC Med* **11**, 181 (2013).
67. Mercer, P.F. *et al.* MMP-9, TIMP-1 and inflammatory cells in sputum from COPD patients during exacerbation. *Respir Res* **6**, 151 (2005).
68. Snelgrove, R.J. Targeting of a common receptor shared by CXCL8 and N-Ac-PGP as a therapeutic strategy to alleviate chronic neutrophilic lung diseases. *Eur J Pharmacol* **667**, 1-5 (2011).
69. De Oliveira, E.O. *et al.* Effect of the leukotriene A4 hydrolase aminopeptidase augmentor 4-methoxydiphenylmethane in a pre-clinical model of pulmonary emphysema. *Bioorg Med Chem Lett* **21**, 6746-6750 (2011).
70. Paige, M. *et al.* Role of Leukotriene A4 Hydrolase Aminopeptidase in the Pathogenesis of Emphysema. *J Immunol* **192**, 5059-68 (2014).

Figure Legends

Figure 1. *Dual LTA_4H activities are functional during Hib infection.* 129/S6 mice were infected with Hib and weight loss assessed daily (**A**). Total cell numbers in the airways (**B**) and lung tissue (**C**) of Hib-infected mice were measured. Bacterial burden was assessed by performing serial dilutions of BALF (**D**) and lung homogenate (**E**) on Brain Heart Infusion agar. The number of neutrophils recruited into the airways (**F**) and lung tissue (**G**) of Hib infected mice was determined by flow cytometry. Mice infected with 1 $x10^7$ Hib were administered control (2A3) or neutrophil depleting (1A8) antibody and neutrophil numbers (**H**) and CFU (**I**) assessed at 24 hours post infection. The concentration of KC (**J**) and MIP-2 (**K**) in the BALF was determined by ELISA. Intracellular epoxide hydrolase activity of BAL cells (**L**). LTB_4 levels in BALF of Hib-infected mice (**M).** Mice infected with 1 $x10^7$ Hib were administered 2A3 or 1A8 antibody and intracellular epoxide hydrolase activity of BAL cells determined at 24 hours post infection (**N**). Amounts of total MMP-9 (**O**) in BALF were assessed by ELISA and MMP-9 gelatinolytic activity (**P**) was assessed by gelatin zymography [representative image depicted: lane 1=naïve; 2=$1x10^6$ 6hrs; 3=$1x10^7$ 6hrs; 4=$1x10^6$ 24hrs; 5=$1x10^7$ 24hrs; 6=$1x10^6$ day 3; 7=$1x10^7$ day 3; 8=$1x10^6$ day 7; 9=$1x10^7$ day 7]. (**Q**) PE activity in BALF at different times after Hib infection. Mice infected with 1 $x10^7$ Hib were administered 2A3 or 1A8 antibody and total MMP-9 levels (**R**) and PE activity (**S**) in the BALF determined at 24 hours post infection. Total LTA_4H levels in BALF were assessed by ELISA at different times post infection (**T**). BALF from different time points post-Hib infection, was incubated with PGP and degradation assessed after 2 hours by mass spectrometry (**U**) or release of free proline (**V**). Mice infected with 1 $x10^7$ Hib were administered 2A3 or 1A8 antibody and PGP degradation by BALF at 24 hrs assessed by mass spectrometry (**W**) or release of free proline (**X**). Data (mean ± S.E.M.) are representative of at least 2 experiments with 5-6 mice per group.*, $P<0.05$; **, $P<0.01$ using Mann-Whitney.

Figure 2. *An absence of LTB_4 signaling does not alter pulmonary inflammation but compromises bacterial clearance.* Blt1-/- mice and WT controls were infected intranasally with 1 $x10^7$ Hib and weight loss assessed daily and expressed as a percentage of the original body mass (**A**). Total cell numbers in the airways (**B**) and lung tissue (**C**) of Hib-infected mice were enumerated. The number of neutrophils recruited into the airways (**D**) and lung tissue (**E**) of Hib infected

mice was determined by flow cytometry. Bacterial burden was assessed by performing serial dilutions of BALF and lung homogenate, at 6 hrs (**F**) and 24 hrs (**G**), on Brain Heart Infusion (BHI) agar plates. Phagocytosis of pHrodo-conjugated Hib by alveolar macrophages (**H**) and neutrophils (**I**) was assessed by flow cytometry. The capacity of WT and blt1-/- alveolar macrophages (**J**) and neutrophils (**K**) to kill Hib was assessed. Hib-infected mice were administered vehicle (PBS), BLT1 antagonist (U-75302) or BLT2 antagonist (LY2552833) and lung neutrophil numbers (**L**) and CFU (**M**) assessed at 24 hours post infection. Data (mean ± S.E.M.) are representative of at least 2 experiments with 5-6 mice per group. *, $P<0.05$; **, $P<0.01$ using Mann-Whitney.

Figure 3. *Hib-infected lta4h-/- mice display augmented illness and pulmonary inflammation.* Lta4h-/- mice and littermate controls were infected intranasally with $1x10^7$ Hib and weight loss assessed daily and expressed as a percentage of the original body mass (**A**). Levels of albumin (**B**) and lactate dehydrogenase (LDH; **C**) in the BALF were assessed by ELISA and enzymatic assay, respectively. Bacterial burden was assessed by performing serial dilutions of BALF (**D**) and lung homogenate (**E**) on Brain Heart Infusion (BHI) agar plates. Total cell numbers in the airways (**F**) and lung tissue (**G**) of Hib-infected mice was enumerated. The number of neutrophils recruited into the airways (**H**) and lung tissue (**I**) of Hib infected mice was determined by flow cytometry. The number of infiltrating monocytes/ macrophages recruited into the airways (**J**) and lung tissue (**K**) of Hib infected mice was determined by flow cytometry. Data (mean ± S.E.M.) are combined from 2 separate experiments with 4-5 mice per group and are representative of 3-4 experiments.*, $P<0.05$; **, $P<0.01$ using Mann-Whitney.

Figure 4. *Failure to degrade PGP drives an exacerbated neutrophilic inflammation in response to Hib infection.* Lta4h-/- mice and littermate controls were infected intranasally with $1 x10^7$ Hib and the concentration of LTB_4 (**A**), KC (**B**), MIP-2 (**C**), TNF-α (**D**) and IL-6 (**E**) in the BALF was determined. The concentration of PGP in BALF was determined by ESI-LC/MS/MS (**F**). BALF from different time points post-Hib infection, was incubated with PGP and degradation assessed after 2 hours by mass spectrometry (**G**) or release of free proline (**H**). Mice were infected intranasally with $1 x10^7$ Hib and 2hrs later treated intranasally with AcPGP or control peptide, AcPGG, and at 24 hrs post infection the number of neutrophils recruited into airways determined by flow cytometry (**I**) and the bacterial burden in the BALF assessed by performing

serial dilutions on Brain Heart Infusion (BHI) agar plates (**J**). Lta4h-/- mice and littermate controls infected intranasally with 1 x10^7 Hib were administered vehicle or RTR peptide and the concentration of PGP in BALF was determined by ESI-LC/MS/MS (**K**). Total cell numbers in the airways (**L**) and lung tissue (**M**) enumerated at 24 hours post infection. Bacterial burden at this time point was assessed by performing serial dilutions of lung homogenate (**N**) on Brain Heart Infusion (BHI) agar plates. The number of neutrophils recruited into the airways (**O**) and lung tissue (**P**) of Hib infected mice was determined by flow cytometry. The concentration of TNF-α (**Q**) and IL-6 (**N**) in the BALF was determined by ELISA. Data (mean ± S.E.M.) are combined from 2 separate experiments with 4-5 mice per group and are representative of 3-4 experiments (A-H) or are representative of at least 2 experiments with 5-6 mice per group (I-R). *, $P<0.05$; **, $P<0.01$ using Mann-Whitney.

Figure 5. *Augmented macrophage inflammation in Hib infected lta4h-/- mice secondary to PGP accumulation and protease discord.* Lta4h-/- mice and littermate controls were infected intranasally with 1x10^7 Hib and levels of total MMP-9 (**A**) and NE (**B**) were assessed by ELISA in the BALF. Levels of MMP-9 mRNA were assessed in lung tissue by real-time PCR (**C**). Bone marrow neutrophils were incubated with media alone, IL-8 or AcPGP and levels of MMP-9 and NE assessed in the supernatant after 15 minutes (**D**). Levels of MMP-12 protein in the BALF were assessed by ELISA (**E**) and MMP-12 mRNA levels in lung tissue assessed by real time PCR (**F**). Lta4h-/- mice and littermate controls infected intranasally with 1 x10^7 Hib were administered vehicle or RTR peptide and the concentration of MMP-9 (**G**), NE (**H**) and MMP-12 (**I**) in the BALF was determined by ELISA at 24 hrs post infection. To determine the role of elastin derived chemotactic fragments in driving cellular recruitment, lta4h-/- mice and littermate controls infected intranasally with 1x10^7 Hib were administered control or BA4 (anti-elastin) antibody and total cell numbers in the airways (**J**) and lung tissue (**K**) enumerated at 4 days post-infection. In the same experiment, the numbers of infiltrating monocytes/ macrophages in the airways (**L**) and lung tissue (**M**) was determined by flow cytometry at 4 days post infection. Data (mean ± S.E.M.) are combined from 2 separate experiments with 4-5 mice per group and are representative of 3-4 experiments (A, B and E) or are representative of at least 2 experiments with 5-6 mice per group (G-M). Data (mean ± SD) are representative of three experiments with at least triplicates (D). *, $P<0.05$; **, $P<0.01$ using Mann-Whitney.

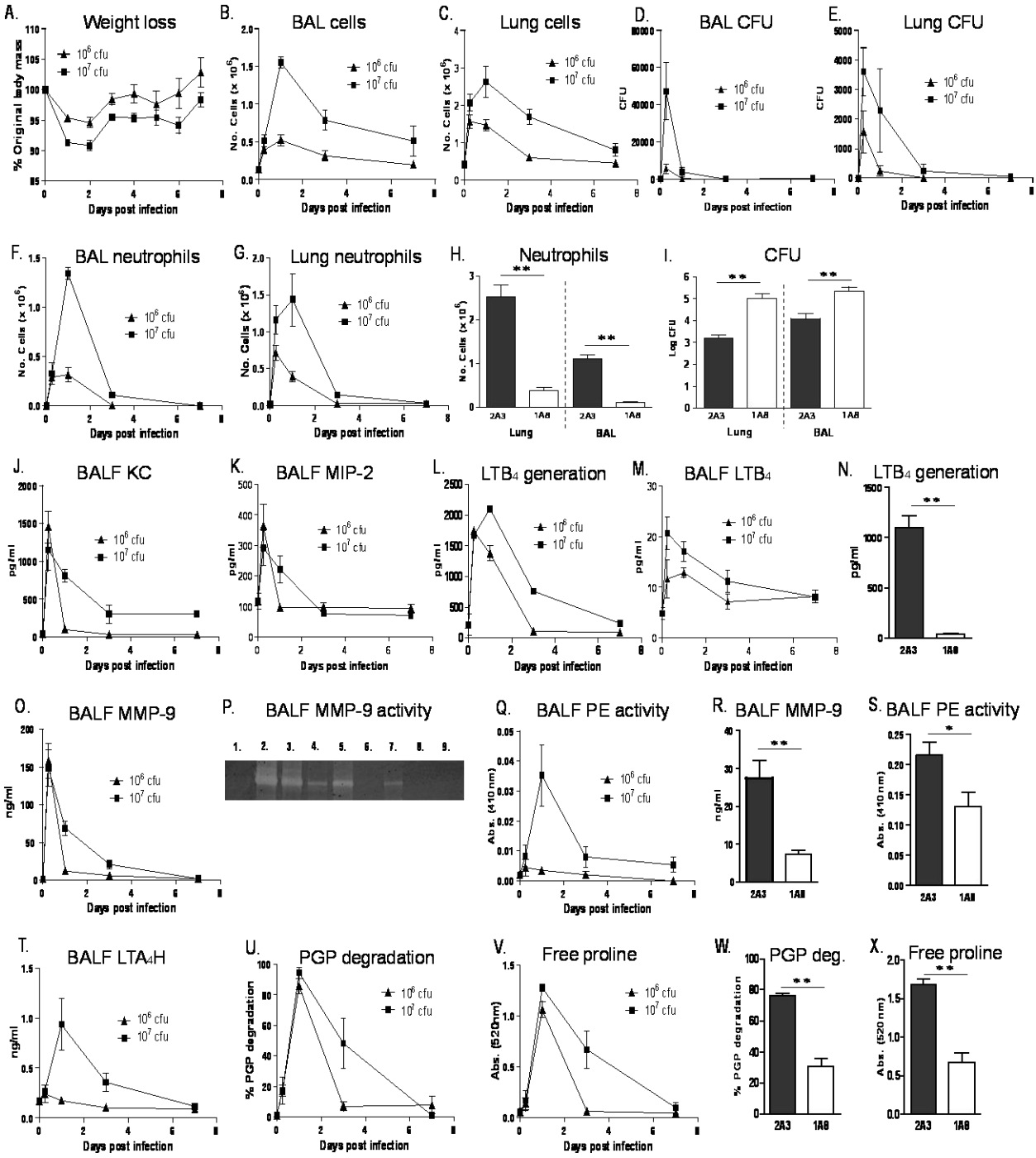
A. Weight loss
% Original body mass
Days post infection
B. BAL cells
No. Cells (x 10^6)
C. Lung cells
D. BAL CFU
CFU
E. Lung CFU
F. BAL neutrophils
G. Lung neutrophils
H. Neutrophils
Lung
BAL
I. CFU
Log CFU
J. BALF KC
pg/ml
K. BALF MIP-2
L. LTB4 generation
M. BALF LTB4
N. LTB4 generation
O. BALF MMP-9
ng/ml
P. BALF MMP-9 activity
1. 2. 3. 4. 5. 6. 7. 8. 9.
Q. BALF PE activity
Abs. (410nm)
R. BALF MMP-9
S. BALF PE activity
T. BALF LTA4H
U. PGP degradation
% PGP degradation
V. Free proline
Abs. (520nm)
W. PGP deg.
X. Free proline
10^6 cfu
10^7 cfu
2A3
1A8

Figure 1.

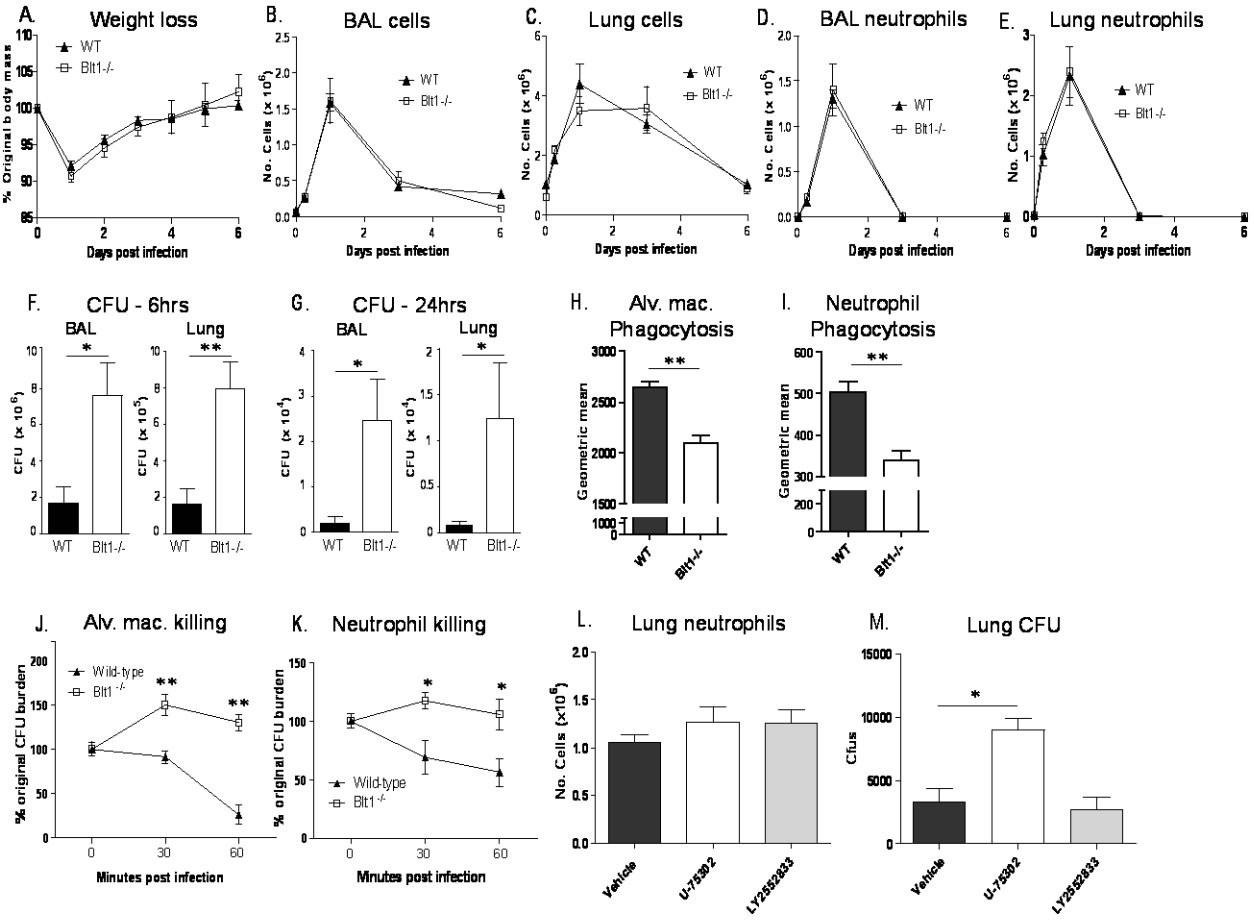
A. Weight loss
% Original body mass
Days post infection
WT
Blt1-/-
B. BAL cells
No. Cells (x 10^6)
C. Lung cells
D. BAL neutrophils
E. Lung neutrophils
F. CFU - 6hrs
BAL
Lung
CFU (x 10^6)
CFU (x 10^5)
G. CFU - 24hrs
CFU (x 10^4)
H. Alv. mac. Phagocytosis
Geometric mean
I. Neutrophil Phagocytosis
J. Alv. mac. killing
% original CFU burden
Minutes post infection
Wild-type
Blt1 -/-
K. Neutrophil killing
L. Lung neutrophils
No. Cells (x10^6)
Vehicle
U-75302
LY255283
M. Lung CFU
Cfus

Figure 2.

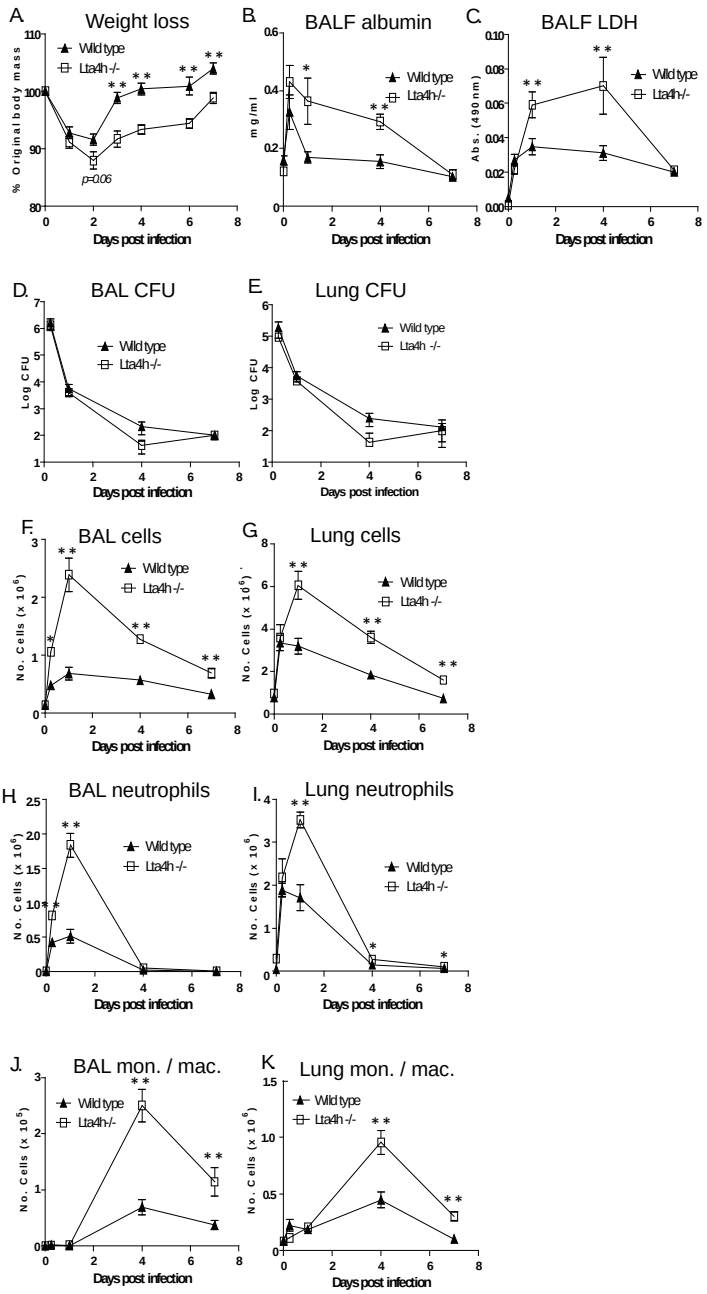
A
Weight loss
% Original body mass
Wild type
Lta4h -/-
p=0.06
Days post infection
B
BALF albumin
mg/ml
Wild type
Lta4h-/-
Days post infection
C
BALF LDH
Abs. (490 nm)
Wild type
Lta4h-/-
Days post infection
D
BAL CFU
Log CFU
Wild type
Lta4h-/-
Days post infection
E
Lung CFU
Log CFU
Wild type
Lta4h -/-
Days post infection
F
BAL cells
No. Cells (x 10^6)
Wild type
Lta4h -/-
Days post infection
G
Lung cells
No. Cells (x 10^6)
Wild type
Lta4h -/-
Days post infection
H
BAL neutrophils
No. Cells (x 10^6)
Wild type
Lta4h -/-
Days post infection
I
Lung neutrophils
No. Cells (x 10^6)
Wild type
Lta4h -/-
Days post infection
J
BAL mon. / mac.
No. Cells (x 10^5)
Wild type
Lta4h-/-
Days post infection
K
Lung mon. / mac.
No. Cells (x 10^5)
Wild type
Lta4h -/-
Days post infection

Figure 3.

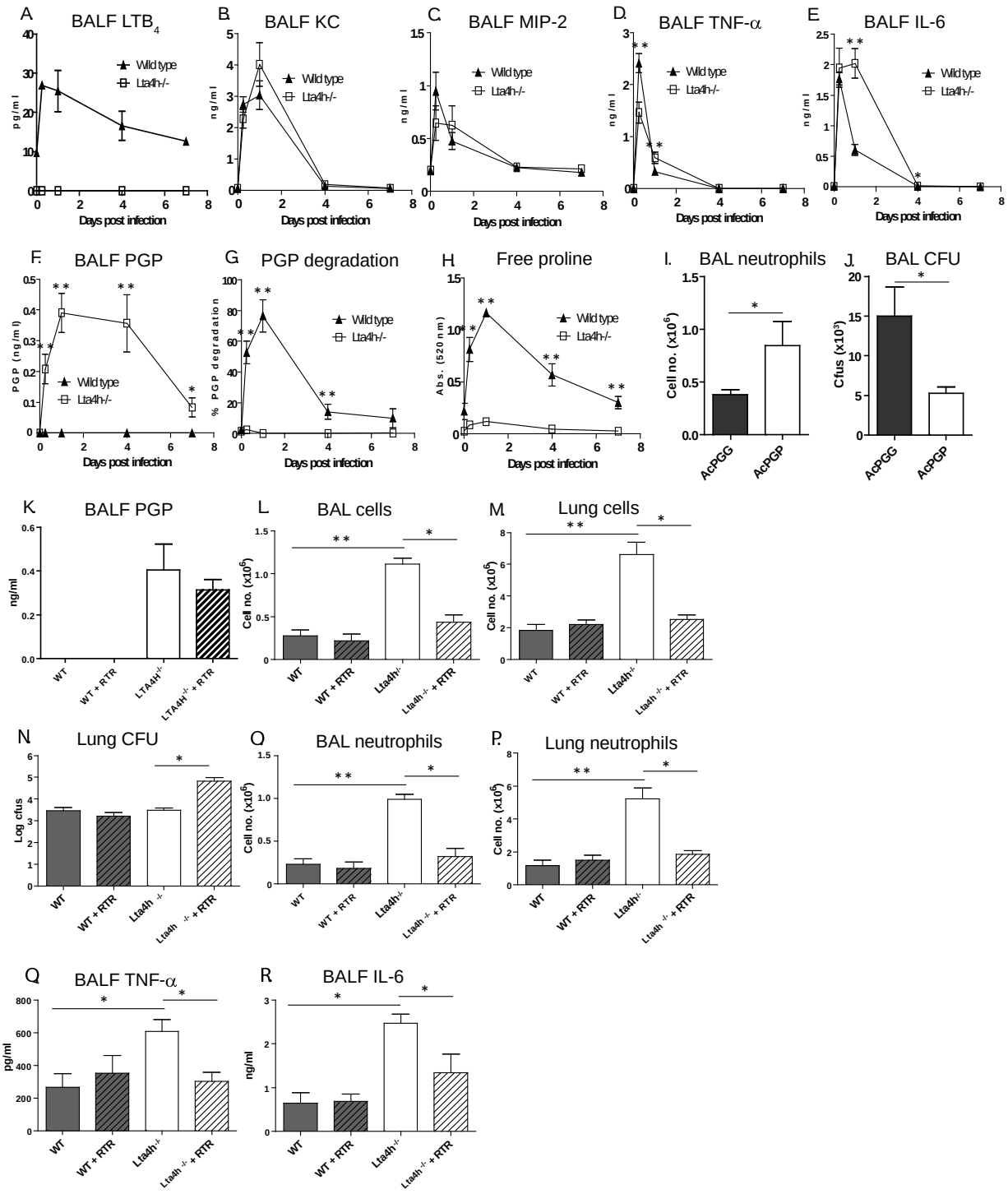
A
BALF LTB4
pg/ml
Wild type
Lta4h-/-
Days post infection
B
BALF KC
ng/ml
C
BALF MIP-2
ng/ml
D
BALF TNF-α
ng/ml
E
BALF IL-6
ng/ml
F
BALF PGP
PGP (ng/ml)
G
PGP degradation
% PGP degradation
H
Free proline
Abs. (520 nm)
I
BAL neutrophils
Cell no. (x10^6)
AcPGG
AcPGP
J
BAL CFU
Cfus (x10^3)
K
BALF PGP
ng/ml
WT
WT + RTR
LTA4H-/-
LTA4H-/- + RTR
L
BAL cells
Cell no. (x10^6)
Lta4h-/-
Lta4h-/- + RTR
M
Lung cells
Cell no. (x10^6)
N
Lung CFU
Log cfus
O
BAL neutrophils
Cell no. (x10^6)
P
Lung neutrophils
Cell no. (x10^6)
Q
BALF TNF-α
pg/ml
R
BALF IL-6
ng/ml

Figure 4.

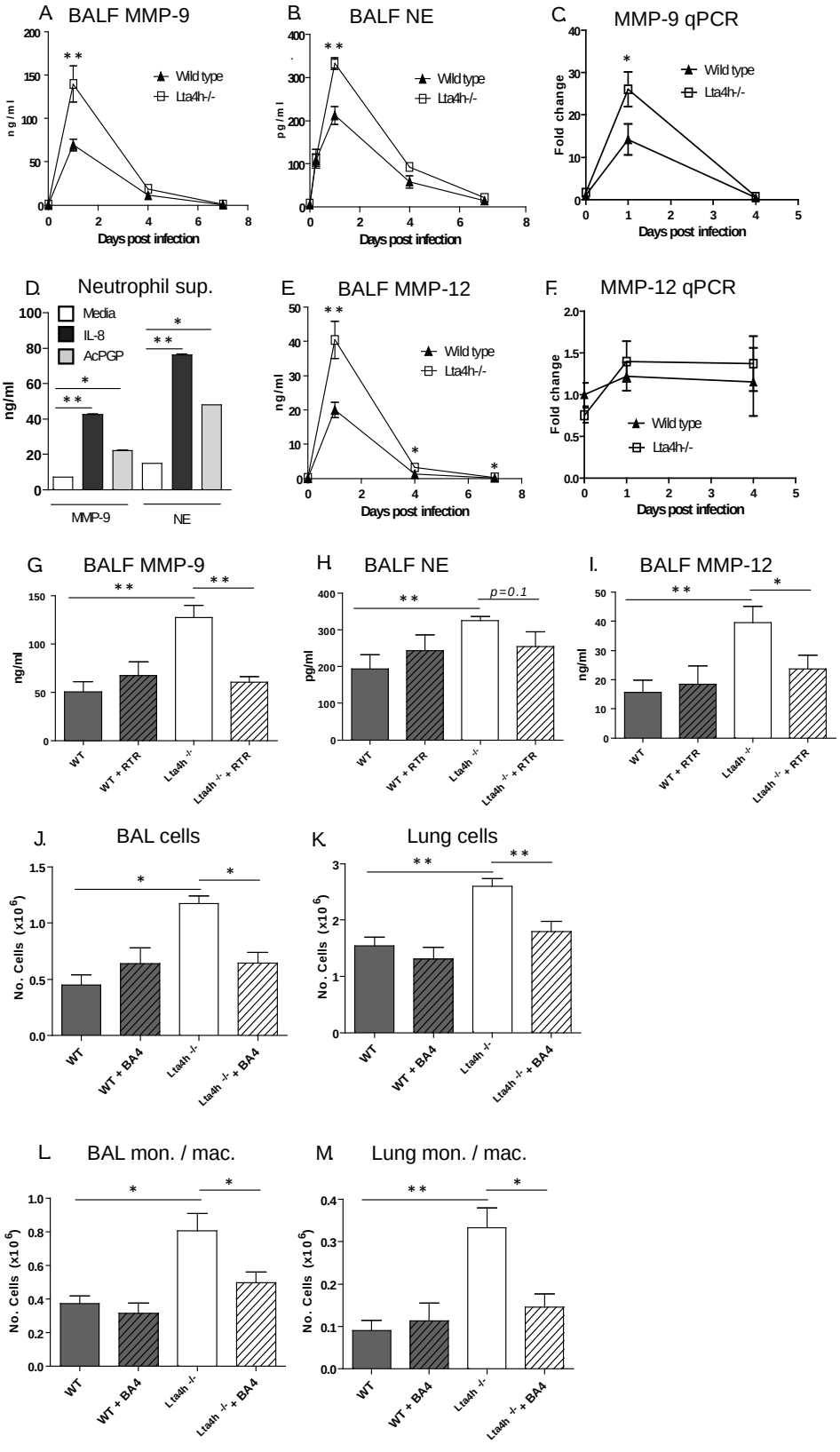
A BALF MMP-9
ng/ml
Wild type
Lta4h-/-
Days post infection
B. BALF NE
pg/ml
C. MMP-9 qPCR
Fold change
D. Neutrophil sup.
Media
IL-8
AcPGP
MMP-9
NE
E. BALF MMP-12
F. MMP-12 qPCR
G. BALF MMP-9
H. BALF NE
p=0.1
I. BALF MMP-12
WT
WT + RTR
Lta4h -/-
Lta4h -/- + RTR
J. BAL cells
No. Cells (x10 6)
K. Lung cells
WT + BA4
Lta4h -/- + BA4
L. BAL mon. / mac.
M. Lung mon. / mac.

Figure 5

Matrikines are key regulators in modulating the amplitude of lung inflammation in acute pulmonary infection

Samia Akthar, Dhiren F. Patel, Rebecca C. Beale, Teresa Peiró, Xin Xu, Amit Gaggar, Patricia L. Jackson, J. Edwin Blalock, Clare M. Lloyd, Robert J. Snelgrove.

Supplementary Material.

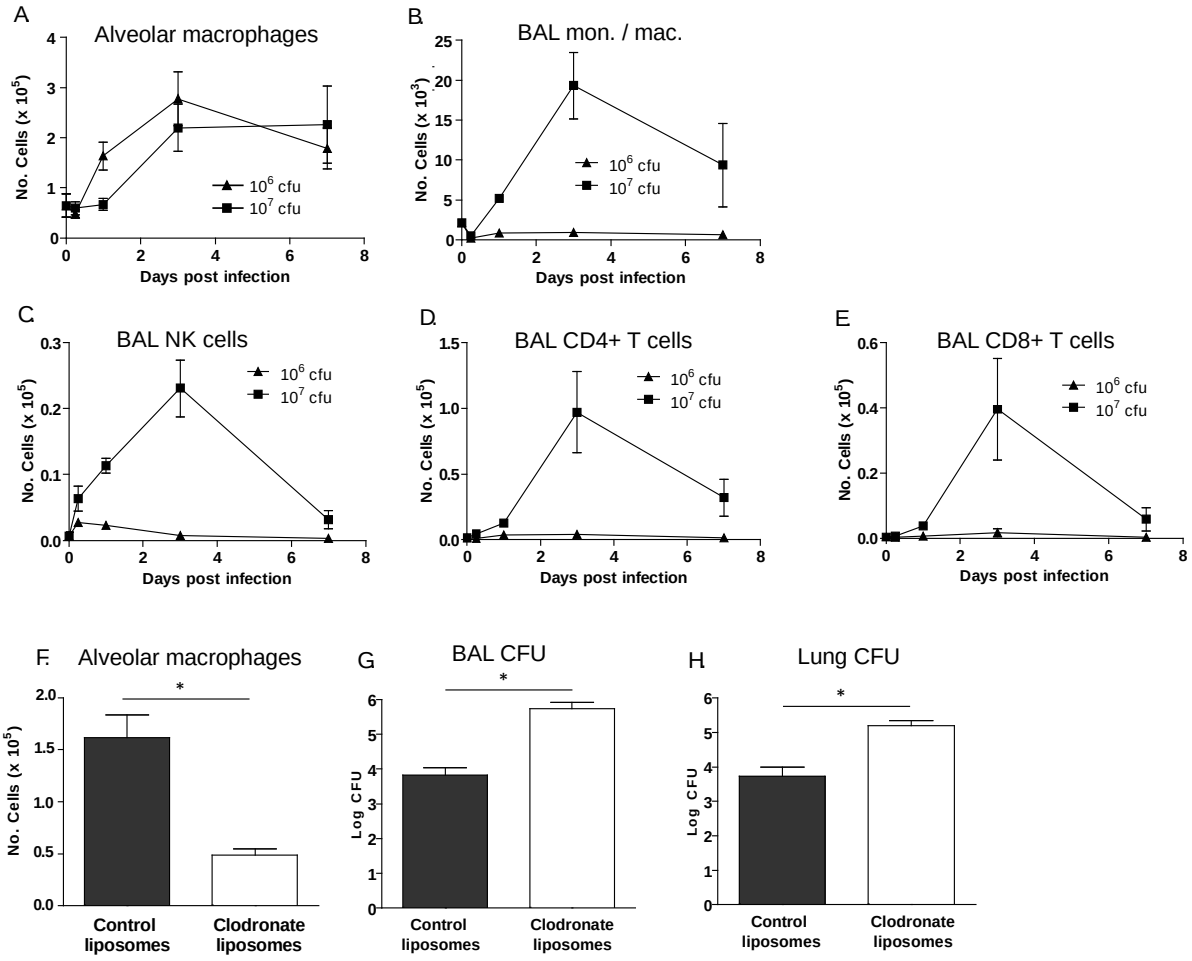

Supplementary figure 1. *Macrophage and lymphocyte response to Haemophilus influenzae b infection.*129/S6 mice were infected intranasally with 1x10^6 or 1 x10^7 *Haemophilus influenzae b* (Hib) and the numbers of alveolar macrophages (**A**), infiltrating monocytes / macrophages (**B**), NK cells (**C**), $CD4^+$ T cells (**D**) and $CD8^+$ T cells (**E**) in the airways of Hib infected mice was determined by flow cytometry. Hib-infected mice were administered control or clodronate liposomes and alveolar macrophage numbers (**F**) and CFU in the airways (**G**) and lung tissue (**H**) assessed at 24 hours post infection. Data (mean ± S.E.M.) are representative of at least 2 experiments with 5-6 mice per group. *, P<0.05; **, P<0.01 using Mann-Whitney.

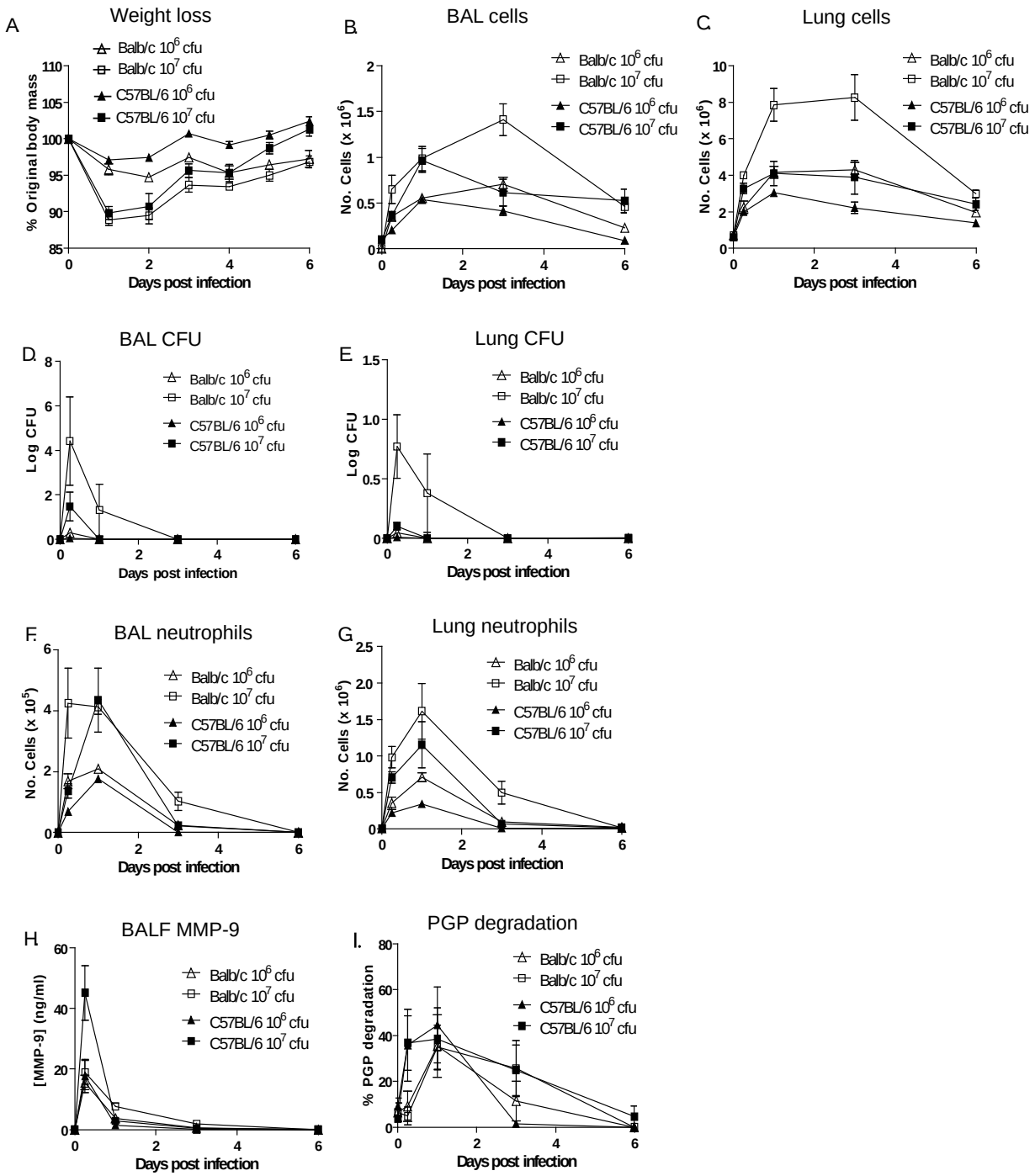

Supplementary figure 2. *Robust, acute pulmonary infiltrate controls Haemophilus influenzae infection in Balb/c and C57BL/6 mice.* Balb/c or C57BL/6 mice were infected intranasally with $1x10^6$ or $1 x10^7$ *Haemophilus influenzae b* (Hib) and weight loss assessed daily and expressed as a percentage of the original body mass (**A**). Total cell numbers in the airways (**B**) and lung tissue (**C**) of Hib-infected mice was enumerated by trypan blue exclusion. Bacterial burden was

assessed by performing serial dilutions of BALF (**D**) and lung homogenate (**E**) on Brain Heart Infusion (BHI) agar plates and counting colony forming units (CFU). The number of neutrophils recruited into the airways (**F**) and lung tissue (**G**) of Hib infected mice was determined by flow cytometry. Amounts of total MMP-9 were assessed by ELISA in the BALF at different times post infection (**H**). BALF from different time points post-Hib infection, was incubated with 4mM PGP and degradation assessed after 2 hours by mass spectrometry (**I**). Data (mean ± S.E.M.) are representative of at least 2 experiments with 5-6 mice per group. *, $P<0.05$; **, $P<0.01$ using Mann-Whitney.

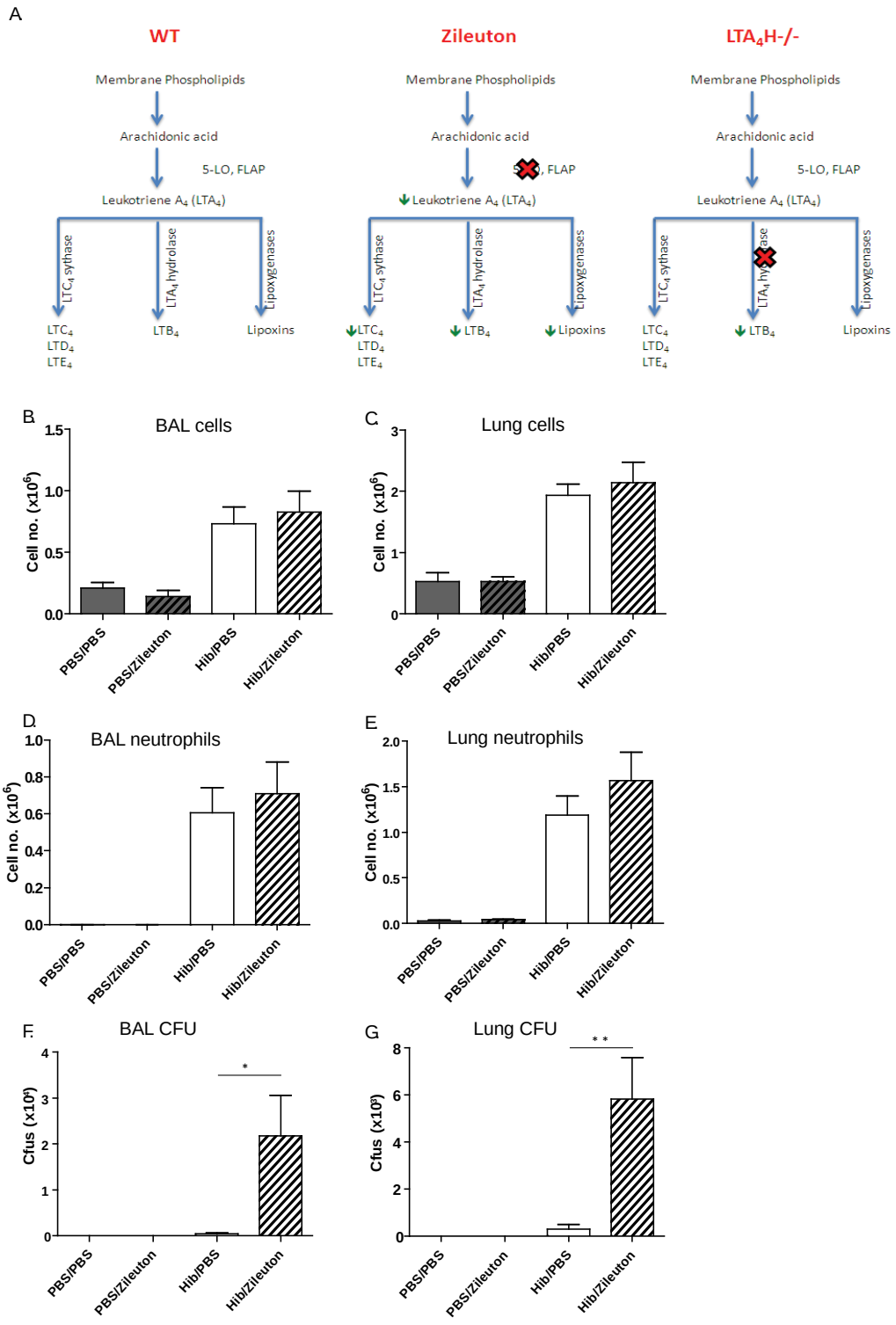

Supplementary figure 3. *5-lipoxygenase inhibition does not alter pulmonary inflammation but compromises bacterial clearance.* (**A**) Arachidonic acid, derived from membrane phospholipids, is converted to leukotriene A_4 (LTA_4) through the action of 5-lipoxygenase (5-LO) and 5-lipoxygenase-activating protein (FLAP). LTA_4 can subsequently be converted to cysteinyl

leukotrienes (LTC_4, D_4, E_4) by the action of LTC_4 synthase, to LTB_4 by the action of leukotriene A_4 hydrolase (LTA_4H) or to lipoxins via the action of lipoxygenases. Zileuton inhibits 5-LO, preventing LTA_4 formation and thus the ensuing generation of cysteinyl leukotrienes, LTB_4 and lipoxins. LTA_4H-/- mice selectively lose the capacity to convert LTA_4 to LTB_4. 129/S6 mice were infected intranasally with 1 $x10^7$ Hib and administered vehicle or zileuton. Total cell numbers in the airways (**B**) and lung tissue (**C**) were enumerated at 24 hours post infection. The number of neutrophils recruited into the airways (**D**) and lung tissue (**E**) of Hib infected mice was determined by flow cytometry. Bacterial burden at this time point was assessed by performing serial dilutions of BALF (**F**) and lung homogenate (**G**) on Brain Heart Infusion (BHI) agar plates. Data (mean ± S.E.M.) are from 5-6 mice per group.*, $P<0.05$; **, $P<0.01$ using Mann-Whitney.

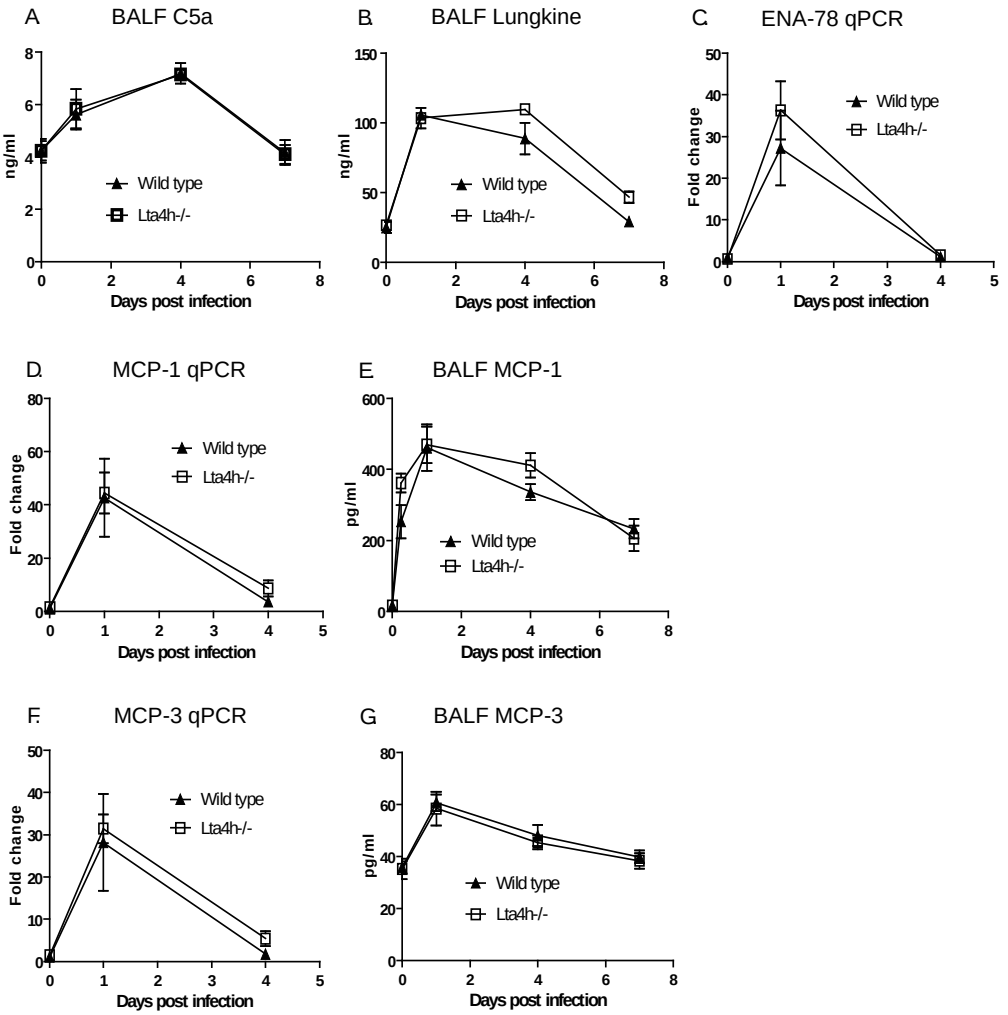

Supplementary figure 4. *Hib-infected lta4h-/- mice display comparable levels of classical neutrophil and monocyte chemoattractants.* Lta4h-/- mice and littermate controls were infected intranasally with $1x10^7$ Hib and levels of C5a (**A**) and lungkine/CXCL15 (**B**) in the BALF were assessed by ELISA. Levels of ENA-78/CXCL5 mRNA were assessed in lung tissue by real time PCR at different times post Hib infection (**C**). Lung mRNA and BALF protein levels of MCP-1/CCL2 (**D** and **E,** respectively) and MCP-3/CCL7 (**F** and **G,** respectively) were determined at different times post Hib infection. Data (mean ± S.E.M.) are representative of at least 2 experiments with 5-6 mice per group (A, B, E and G) or are from a single experiment with 5 mice per group (C, D and F). *, $P<0.05$; **, $P<0.01$ using Mann-Whitney.

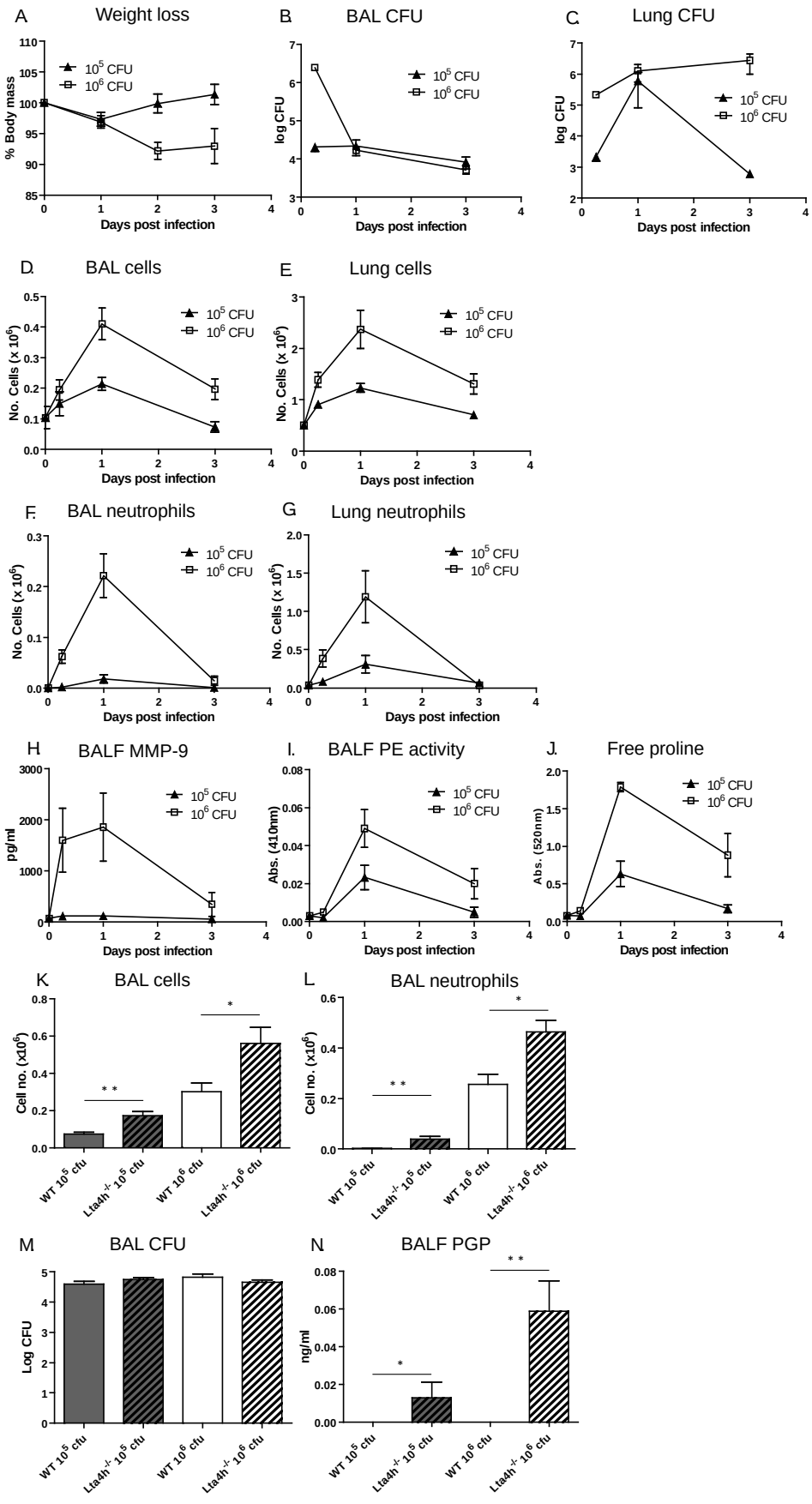
A
Weight loss
% Body mass
Days post infection
B
BAL CFU
log CFU
Days post infection
C
Lung CFU
log CFU
Days post infection
D
BAL cells
No. Cells (x 10^6)
Days post infection
E
Lung cells
No. Cells (x 10^6)
Days post infection
F
BAL neutrophils
No. Cells (x 10^6)
Days post infection
G
Lung neutrophils
No. Cells (x 10^6)
Days post infection
H
BALF MMP-9
pg/ml
Days post infection
I
BALF PE activity
Abs. (410nm)
Days post infection
J
Free proline
Abs. (520nm)
Days post infection
K
BAL cells
Cell no. (x10^6)
WT 10^5 cfu
Lta4h-/- 10^5 cfu
WT 10^6 cfu
Lta4h-/- 10^6 cfu
L
BAL neutrophils
Cell no. (x10^6)
WT 10^5 cfu
Lta4h-/- 10^5 cfu
WT 10^6 cfu
Lta4h-/- 10^6 cfu
M
BAL CFU
Log CFU
WT 10^5 cfu
Lta4h-/- 10^5 cfu
WT 10^6 cfu
Lta4h-/- 10^6 cfu
N
BALF PGP
ng/ml
WT 10^5 cfu
Lta4h-/- 10^5 cfu
WT 10^6 cfu
Lta4h-/- 10^6 cfu

Supplementary figure 5. *Streptococcus pneumoniae infected lta4h-/- mice display augmented pulmonary inflammation.* 129/S6 mice were infected intranasally with $1x10^5$ or $1x10^6$ *S. pneumoniae* and weight loss assessed daily and expressed as a percentage of the original body mass (**A**). Bacterial burden was assessed by performing serial dilutions of BALF (**B**) and lung homogenate (**C**) on Columbia blood agar. Total cell numbers in the airways (**D**) and lung tissue (**E**) of *S. pneumoniae* infected mice was assessed. The number of neutrophils recruited into the airways (**F**) and lung tissue (**G**) of *S. pneumoniae* infected mice was determined by flow cytometry. Amounts of total MMP-9 in BALF were assessed by ELISA (**H**) at different times post infection. (**I**) PE activity in BALF at different times after *S. pneumonia* infection was determined by change in absorbance at 410 nm following cleavage of p-nitroaniline from PE specific substrate ZGP-pNA. BALF from different time points post-Hib infection, was incubated with PGP and degradation assessed after 2 hours by release of free proline (**J**). Lta4h-/- mice and littermate controls were infected intranasally with $1x10^5$ or $1 x10^6$ *S. pneumoniae* and total cell numbers in the airways enumerated at 24 hours post infection (**K**). The number of neutrophils recruited into the airways of *S. pneumoniae* infected mice was determined by flow cytometry (**L**). Bacterial burden was assessed by performing serial dilutions of BALF on Columbia blood agar plates (**M**). The concentration of PGP in BALF was determined by ESI-LC/MS/MS (**N**). Data (mean ± S.E.M.) are from 5-6 mice per group. *, $P<0.05$; **, $P<0.01$ using Mann-Whitney.

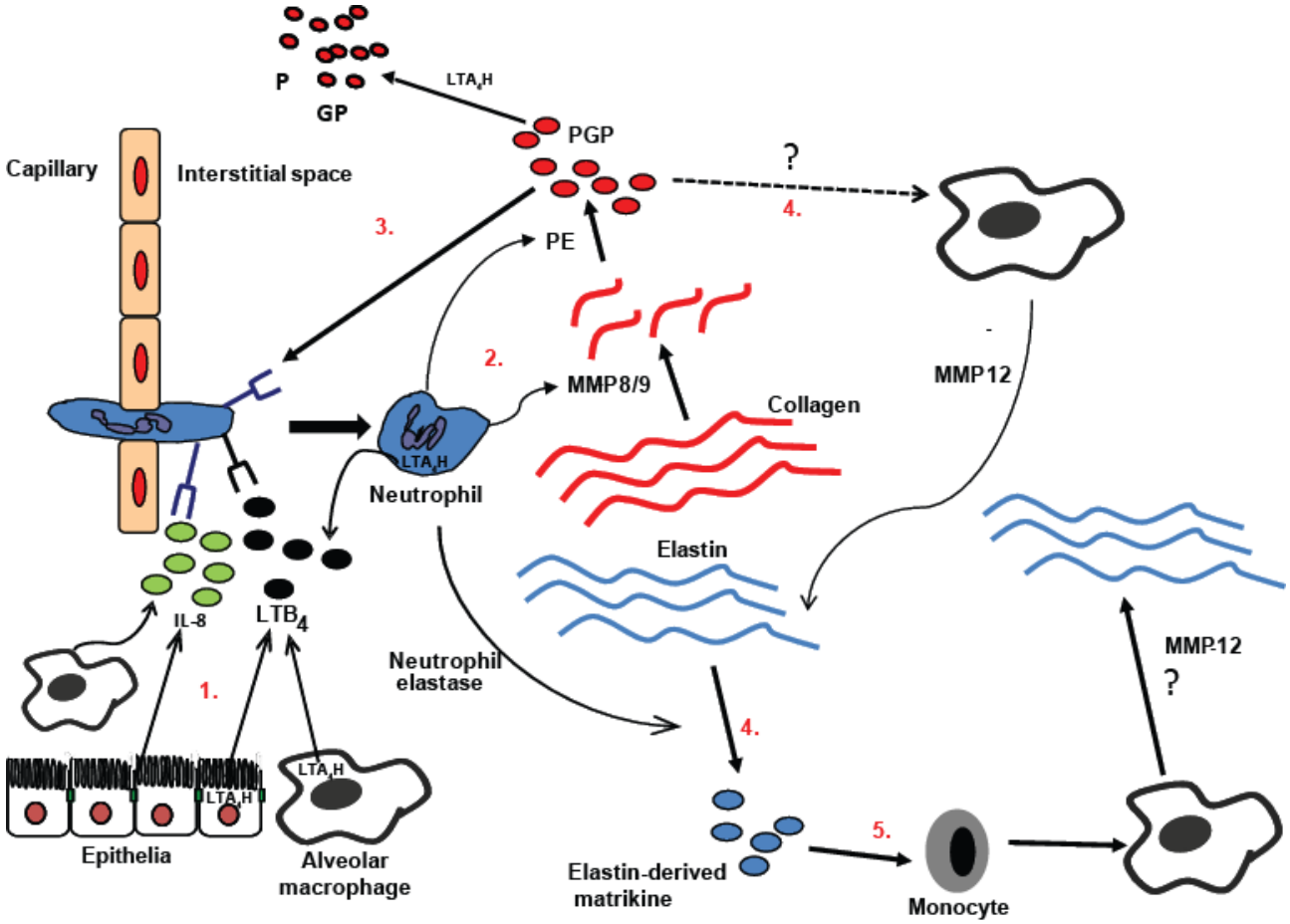

Supplementary figure 6. *A failure to degrade PGP leads to a protease-matrikine discord that exacerbates inflammation.* **1.** In response to infection or injury, pulmonary cells release classical neutrophil chemoattractants, such as IL-8 and LTB_4, leading to the recruitment of neutrophils from the vasculature and into the lung tissue. **2.** Recruited neutrophils release an array of proteases and the concerted actions of MMP-8/9 and PE target extracellular matrix collagen to yield the matrikine PGP. **3.** A failure to degrade PGP by LTA_4H enables it to promote further neutrophil recruitment and release of MMPs/PE with ensuing further generation of PGP – a feed forward mechanism to promote a vicious circle of neutrophilia. **4.** PGP also elicits the release of NE from neutrophils and, indirectly, the release of MMP-12 from alveolar macrophages. These elastases target extracellular matrix elastin to yield elastin-based matrikines that are chemotactic for monocytes. **5.** These chemotactic elastin fragments promote monocyte recruitment. Monocytes mature into tissue macrophages that may produce more MMP-12 to target elastin and generate further matrikines.